

Estimation of Frequency Control Performance Index

by

Zubaer Bin Zahid

A Thesis submitted to the Faculty of Graduate Studies
The University of Manitoba
in partial fulfillment of the requirements of the degree of
MASTER OF SCIENCE

Department of Electrical and Computer Engineering
Faculty of Engineering
University of Manitoba

Abstract

This thesis proposes two methods to estimate transfer function models using System Identification technique that can be used to estimate Control Performance Standard 1 (CPS1) index. The first method is applicable when a load-frequency time domain simulation system of an interconnected power system for estimation of CPS1 is available. This method models an accurate approximate equivalent power system external to a system under consideration. The second method is applicable when a time domain simulation model for estimation of CPS1 is not available. This method uses System Identification technique to model two transfer functions to produce necessary data for the estimation of CPS1. The necessary up-to-date data for System Identification can be obtained from a practical power system dynamic simulation model. The developed models are used to estimate CPS1. The research described in this thesis also shows the applicability of a previously developed method of estimating CPS1 in a practical power system. The techniques, methodology and results presented in this research should provide useful information for operating and planning of power systems.

Acknowledgements

I am using this opportunity to express my gratitude to everyone who supported me throughout the course of this M.Sc. research and preparation of this thesis. I am thankful for their aspiring guidance, invaluable constructive criticism and friendly advice during the research work. I am sincerely grateful to them for sharing their truthful and illuminating views on a number of issues related to the research.

I express my warm thanks to Dr. Annakkage my academic supervisor and Dr. Bagen my industrial supervisor for their support and guidance.

Table of Contents

1	Introduction	1
1.1	Background	1
1.2	Problem Formulation	4
1.3	Motivation for the Research	6
1.4	Objectives of the Research	7
2	Active Power and Frequency Control	9
2.1	Introduction	9
2.2	Overview of a Typical Power System	9
2.3	Power System Control	11
2.4	Active Power and Frequency Control	13
2.4.1	Response of a Generator to a Load Change	13
2.4.2	Load Response to Change in Frequency	15
2.4.3	Governor Speed Control	17
2.4.4	Combined Speed Regulating Characteristic	21
2.4.5	Frequency Control	23
2.4.6	Tie Line Bias Control	25
2.5	Summary and Conclusions	28

3	NERC Control Performance Standard	29
3.1	Introduction	29
3.2	Types of Control Performance Standards	30
3.3	Control Performance Standard 1	30
3.3.1	Calculation Process of Compliance Factor	33
3.3.2	Data Reporting	36
3.4	Components of CPS1	37
3.5	Summary and Conclusions	43
4	Application of System Identification Technique	44
4.1	Introduction	44
4.2	System Identification	45
4.2.1	Classification of the System Identification	46
4.2.2	System Identification Procedure	47
4.3	Estimation of Transfer Function Models Using MATLAB System Identification Toolbox	49
4.3.1	Model Objects	50
4.3.2	Input/Output Data	53
4.3.3	Identifying Transfer Function Models	55
4.4	Modeling an Enhanced External System for a Time Domain Simulation of an Interconnected Power System	60
4.4.1	Proposed Methodology	60
4.4.2	Load Frequency Simulation Model	61
4.4.3	External System Modeling For a Practical Power System	64
4.4.4	External System Model Testing and Observation	66

4.5	Modeling Transfer Functions to Obtain Δf and ΔP for a Practical Power System for the Estimation Purpose of CPS1	75
4.5.1	Proposed Methodology	75
4.5.2	Application of the Proposed Methodology	76
4.5.3	Modeling the Transfer Functions	78
4.6	Summary and Conclusions	81
5	Estimation of Control Performance Standard 1 (CPS1)	83
5.1	Introduction	83
5.2	Relationship Between a Single Step Load Change With CF and It's Components	84
5.2.1	Relationship Between Δf_{1M} , ΔP_{1m} , and the Magnitude of a Single-Step-Load-Change	85
5.2.2	Relationship of Single-Step-Load-Change With CF_{1M}	88
5.3	Significant Period of CF_{1M}	90
5.4	Estimation of CF and It's Components for a Multi-Step-Load-Change . .	91
5.4.1	Estimation of CF_{1M} When a Time Domain Simulation Model is Available	91
5.4.2	Estimation and Validation of CF_{1M} and CPS1 Using Data from Transfer Function Models	94
5.5	Summary and Conclusions	98
6	Summary and Conclusions	99
6.1	Summary	99
6.2	Contributions	101
6.3	Future Work	102

A	System Identification	104
A.1	Types of System Identification Technique	104
A.2	Least Squares Theory	107
A.3	Statistical Properties of Least Squares Estimators	110
A.4	Transfer Function Identification	114
A.4.1	General Concepts	114
A.4.2	Some Typical Impulse Response Functions	117
A.4.3	The Cross Correlation Function and Transfer Function	118
A.4.4	The Relationship Between the Cross-Correlation Function and the Transfer Function	119
A.4.5	Construction of Transfer Function Models.	121
A.5	About PSS/E Simulation Program	127

List of Tables

3.1	Range of CF and CPS1	41
3.2	CPS1 value in different conditions	42
5.1	CF_{1M} values	90
5.2	Comparison of CPS1 Values When the First Method is Applied	94
5.3	CF_{1M} Values used for PDF Method	96
5.4	Comparison of CF_{1M} Values When the Second Method is Applied	97
5.5	Comparison of CPS1 Values When the Second Method is Applied	97
A.1	Impluse reponse weights	116
A.2	Transfer function for $r=0$	117
A.3	Transfer function for $r=1$	118

List of Figures

2.1	Schematic Diagram Illustrating Different Levels of Power System Control.	12
2.2	Simplified Diagram of an Isolated Load Supplied by a Generator.	14
2.3	Block Diagram Showing the Relationship Between the Frequency, System Inertia and Power Mismatch.	15
2.4	Block Diagram Including the Load Damping Effect.	16
2.5	Reduced Block Diagram Including the Load Damping Effect.	17
2.6	Representation of a Speed Governor in Block Diagram.	18
2.7	Generator With a Speed Governor Supplying an Isolated Load.	18
2.8	An Isochronous Governor Schematic Representation.	19
2.9	Speed Droop Governor Schematic Diagram.	20
2.10	Speed Droop Governor With Reduced Governor Transfer Function. . . .	21
2.11	System Equivalent Representation with Transfer Function.	22
2.12	Block Diagram of Two Area Interconnected Power System With AGC. .	27
3.1	The relationship of CPS1 with CF.	37
3.2	$\sum(\Delta P_{1M} * \Delta f_{1M})$ in different quadrants	40
4.1	System Identification Procedure Flow Chart.	48
4.2	Interface of MATLAB System Identification Toolbox.	50
4.3	Transfer Function Identification Dialogue Box.	57

4.4	Selection of Number of Poles and Zeros for the Transfer Function Estimation.	58
4.5	Manitoba Hydro Load-Frequency Model.	62
4.6	Model of the External System	63
4.7	External System Modeled Using the Proposed Methodology	65
4.8	Measured Frequency Deviation in Per Unit.	67
4.9	Measured Tie Line Power in Per Unit.	67
4.10	Tie Line Power Deviation in Per Unit (generated from the previous model).	68
4.11	Tie Line Power Deviation in Per Unit (generated using the proposed methodology).	68
4.12	Comparison of Tie Line Powers (all quantities are in per unit).	69
4.13	Three Step Load Changes.	70
4.14	Frequency Deviation Following Three Step Load Changes.	70
4.15	Tie Line Power Deviation Following Three Step Load Changes.	71
4.16	Eight Step Load Changes.	72
4.17	Frequency Deviation Following Eight Step Load Changes.	72
4.18	Tie Line Power Deviation Following Eight Step Load Changes.	73
4.19	Input and Output From The Transfer Function Model is Plotted Together in the Case of New External System Model	74
4.20	Estimated and Original Frequency Deviation Data Curve Comparison. .	80
4.21	Estimated and Original Tie Line Power Deviation Data Curve Comparison.	80
5.1	ΔF^i For Load Increase in Manitoba Area.	86
5.2	ΔP^i For Load Increase in Manitoba Area.	87
5.3	Clock-One-Minute-Average Value of Δf for the First Minute.	88
5.4	Clock-One-Minute-Average Value of ΔP for the First Minute.	88
5.5	CF_{1M} for the First Minute for Different Load Changes.	89

5.6	Twenty-Step-Load-Change.	92
5.7	Random Load Change Provided to the System.	95
5.8	Frequency Deviation for 20 Step Load Changes.	95
5.9	Tie Line Power Deviation for 20 Step Load Changes.	96
A.1	An n-parameter Linear System.	107
A.2	A Dynamic Transfer Function System.	115

Chapter 1

Introduction

1.1 Background

Electricity is a distinct commodity in which the generation and distribution must be matched at all instants, at all times. Unlike many other forms of energy, electricity cannot be stored, as a result it cannot be produced in advance for future demand or use. Hence it is a necessity to use a practical control system to ensure that the generation is meeting the continuously changing load demand for both real and reactive power at all times. Real power is closely related to frequency control. As a result, in order to maintain the system frequency to an acceptable value, the real power generation should be maintained to be equal to the real power consumption of the loads and losses. Mismatch between the real power generation and real power load consumption will result in frequency deviation. In North American power system operation frequency deviation of a small percentage from its nominal value is considered as acceptable [1]. Large frequency deviation can affect power system operation which could even lead to system collapse. Hence for a satisfactory performance of the power system it is desired that the system frequency should remain to its nominal value most of the time.

In an interconnected power system with two or more independently controlled areas, each control area is responsible for maintaining a pre-determined power interchange with the other neighboring areas. Hence in each controlling area individual generation has to be maintained and controlled in order to meet the scheduled power interchange. In general the control of frequency and generation is referred to as Load Frequency Control (LFC)[2]. The main purpose of LFC is to keep the frequency to its nominal value (60 Hz) and net inter area tie line power flow to the scheduled values. This is important for an interconnected power system to operate reliably and safely.

North American electrical power industry began its large scale operation in the earlier part of 20th century [1]. This was beneficial to the customers in a way that, it requires the utility companies to deliver power to the consumers in an effective and efficient way to gain economies of scale. This resulted in the utility companies forming 'power pools' with the other nearby utility companies. The objective was to collaborate with each other to schedule generation in a cost effective manner, which was helpful to reduce the operational cost for all the members of that pool. In 1927, the world's first continuous power pool resembling modern national grid was formed [3]. Three companies called the Public Service Electric and Gas Company, Philadelphia Electric Company and Pennsylvania Power & Light Company, formed the Pennsylvania-New Jersey Interconnection [3]. Thereafter a large number of isolated bulk electricity producers and suppliers started to become interconnected with each other and the interconnections became geographically larger. Eventually the transmission system of electric utilities in Canada and United States interconnected into a large power grid, known as the "North American Power Systems Interconnection", consisting of four interconnections [4]: the Western intercon-

nection, the Eastern interconnection, the Electric Reliability Council of Texas (ERCOT) interconnection and the Quebec interconnection. Among them, the Eastern Interconnection is the largest one, which covers most of Eastern North America except most of Texas. The second largest one is the Western Interconnection which covers most of Western North America and has several High Voltage Direct Current (HVDC) connections to the Eastern interconnection. The ERCOT interconnection also has one HVDC link with the Eastern interconnection and covers most of the State of Texas. Quebec interconnection covers the province of Quebec in Canada, and it is operational as a separate interconnection. It has an HVDC connection with the Eastern interconnection.

An Interconnection consists of two or more "Control Areas" among which the monitoring and controlling function is deconcentrated [4]. Control areas are connected to each other via tie lines. In North America control areas in an interconnection are synchronized at an average frequency of 60Hz. Therefore, each control area is responsible for maintaining that nominal frequency, while ceaselessly manipulating each of its generation to meet the net scheduled interchange bindings. The nominal frequency is also known as the scheduled power system frequency and is the frequency that a power system or an interconnected system is always trying to achieve[5]. The net scheduled interchange is the net power flow that a control area is supposedly to maintain on its area tie lines[5]. All the control areas are subjected to get the benefits of an interconnection equally. Control areas should contribute in an even manner. As an example, if one area is continuously unable to support neighboring areas but only receiving the support from others should be penalized. In order to be consistent in dealing with these kinds of situations there should be necessary standards to regulate the control area performance of interconnected systems.

In the North American utilities, control area performance has been assessed by the North American Electric Reliability Corporation (NERC)[4]. NERC defines the reliability standards applicable for the eight regional entities which are known as Regional Reliability Councils. NERC and all the regional councils cover the entire interconnection of United States of America, Canada and a portion of Baja California in Mexico [6]. The province of Manitoba in Canada is under Midwest Reliability Organization (MRO), which is one of the NERC's regional reliability councils within Eastern Interconnection.

1.2 Problem Formulation

For many years members of NERC used the Control Performance Criteria (CPC) as a measure for the control performance. But in the year of 1997, it came to attention that they were lacking technical justification. In many cases, while evaluating the performance of the power system, engineers have felt that even if a power system fulfills the good control area performance criteria, it does not reflect an actual good interconnected system operation and vice versa [7]. Therefore, NERC has developed and enforced a Reliability Standard BAL-001-1 Real Power Balancing Control Performance [6] in order to assure safe and reliable operation of North American interconnected electric power systems. The BAL-001-1 replaces the CPC with two new standards called the Control Performance Standard (CPS) and Disturbance Control Standard (DCS)[8]. CPS consists of two indices, known as Control Performance Standard 1 (CPS1) and Control Performance Standard 2 (CPS2) [7]. CPS1 puts a limit on the average of a function which consists of Area Control Error (ACE) and interconnection frequency deviation from the scheduled value of 60 Hz[7]. ACE is the tie line power deviation biased with frequency deviation. CPS2 on the other hand sets a limit on ten minute average value of ACE[7].

NERC standard BAL-001-0 requires that each Balancing Authority shall achieve, as a minimum requirement of 100% for CPS1 and 90% for CPS2 to be in compliance [7]. Regional Reliability Councils who are working with NERC are responsible for observing compliance of the registered control areas within their regional boundaries. The areas failing to comply with the standards would be penalized[6].

The CPS1 and CPS2 are acceptable measures of the interconnected area's control performance for many reasons. The following are the merits of CPS indices as compared to the older metrics that were used before 1997 [9].

- CPS indices has a technically defensible basis, developed from logical and mathematical relations between ACE and frequency deviation of an interconnection.
- Application of CPS indices is possible to almost all types of areas without considering their size or other system parameters.
- To comply with CPS indices requires less unit maneuvering, which results in significant savings in fuel costs and unit depreciation.
- CPS indices can be used to effectively evaluate both primary and secondary type of controls which are used in a power system to maintain the balance between the generation and consumption (load).

This thesis focuses on evaluating the CPS1 including details of its definition and properties.

1.3 Motivation for the Research

Power utility companies keep record of many of the power system parameters including the frequency and tie line power. CPS1 in an area is estimated using the recorded values of the corresponding area's frequency deviations and the deviations of tie line power flows during system operation [4].

In order to estimate the CPS1 value for a future time, a load forecast can be used to calculate the frequency deviation and tie line power deviation of inter area power flow using time domain simulation.

In most cases the load forecast is available as a probability density function (or a histogram of probability) of load level [10] [11]. A random load pattern can be produced from the load probability density function that can be used in the time domain simulation for the calculation purpose of CPS1.

It is a time consuming process to calculate the CPS1 through time domain simulation or using recorded system data. From the recorded data it is only possible to calculate the CPS1 for past time. Even though the calculated CPS1 values are accurate, it does not provide adequate detailed insight of what the calculation process comprise of [10] [11].

This research focuses on the following areas to enhance the CPS1 evaluation which comes from the necessity of extending the estimation process for larger system assessment:

- Calculation of CPS1 from the past system data (currently used by utilities) is only possible for the past time thus cannot be used for forecasting.
- Estimation of CPS1 by carrying out a time domain simulation is a time consuming process and may not be very effective for operational and planning or AGC tuning

purposes.

- Estimation of CPS1 using probability distribution of load change is tested only in a simple system.

1.4 Objectives of the Research

The deregulated electricity market, with competition enhancement is a demand of the situation to have rules which would fulfill the objectives of having an efficient market with necessary amount of power system security [12]. In the power system planning and operation estimation of the CPS1 ahead of time is advantageous for various reasons. In recent times, the electric power industry is experiencing tremendous changes. For example: the increased utilization of various energy sources, various changes in electric market, and the introduction of mandatory regulatory standards such as BAL-001-1; it has become necessary and important to develop a process to obtain and predict the frequency control performance standard index - CPS1 ahead of time so that the utility can meet the related existing and potential future standards in the most efficient manner.

Usually in the power system simulation the total power system model is simulated to gather the time domain data necessary for the CPS1 calculation [13]; which is again a time consuming process. This thesis proposes an approach to obtain the related necessary simulation data for estimation of CPS1, without running a detailed power system simulation. In this context system identification method has been used to model transfer functions using data obtained from a practical power system simulation model. These transfer functions can be used by feeding load change distribution data as input to reproduce the frequency deviation and tie line power deviation data. This thesis also proposes

another approach which uses system identification technique to more accurately model an equivalent power system external to the system under consideration for a time domain simulation system which can be used to estimate CPS1.

Objectives of the research described in this thesis are:

- Develop a time domain simulation model which is external to a system under consideration using System Identification technique.
- Develop a method to estimate necessary transfer function models to obtain required data for the calculation of the CPS1 given the probability distribution of load change.
- Apply and validate the PDF method of estimation of CPS1 for a practical interconnected power system.

In order to achieve the above objectives, the following works has been done.

- Study and analysis of the requirements of NERC BAL-001-0 standard, to gain knowledge of the CPS1 index.
- Analysis of each component of CPS1 to understand the concept and relation of each component in the performance of a power system and its impact on CPS1 calculation with respect to control of tie line power flow and system frequency.
- Study of the System Identification method.

Chapter 2

Active Power and Frequency Control

2.1 Introduction

The literature on interconnected power system operation and frequency control performance and its standards are reviewed in this chapter. Generator and load response to a load change is described. Types of frequency control are discussed. Some discussions on Automatic Generation Control and Tie-Line Bias Control are also presented along with their importance in interconnected power systems.

2.2 Overview of a Typical Power System

Two important parameters of AC power systems are frequency and voltage. It is desired to have both of these parameters within a desired bound for successful operation of a power system. A multiple level of control mechanism is deployed to meet the above requirements in a typical power system, various types of complex control equipment and algorithms can be engaged in this purpose. Generation, transmission and distribution are the main functional zones of a power system. The generating stations, which can be

of various types, produce the electricity and it is transmitted through the transmission network. The transmission network consists of short, medium and long distance lines which makes up the transmission, sub-transmission and distribution grids.

Generators are one of the main pieces of equipment for generating power by converting other forms of energy, typically mechanical energy input to electrical energy output. Energy can be obtained using different types of sources, including natural gas, sunlight, steam, water, wind etc. Energy from wind, running water, steam or gas is converted into mechanical energy by using a turbine that drives the generator. Different type of turbines such as, steam turbines, hydraulic turbines, gas turbines or wind turbines are generally known as prime movers.

A transmission system is used to deliver the power from the generating plant to the consumer end through transmission network. Consumer loads are fed through the distribution system. Transmission lines may connect the other power utilities in the surrounding area; this enables economical power transfers during normal operating condition and contributing to support each other during emergency conditions [1].

Customers are mostly connected at the transmission, sub-transmission and distribution level. The power consumers are commonly called "load". There are various types of load such as industrial, commercial and residential loads. The big industrial loads are usually directly connected to the main transmission network system. Comparative smaller industrial loads are fed through the sub-transmission network. Other smaller industrial loads are served from primary distribution network and commercial and residential loads get their power from secondary distribution network.

2.3 Power System Control

Figure 2.1, shows different levels of a power system from generation to transmission and includes various controls closely related to each subsystem [14]. The objective of a control system in the power system is quite simple: it is to generate and deliver active and reactive power reliably and economically to the consumers and to maintain voltage, frequency and other important system variables to its safe limit. The active power is sensitive to frequency change and reactive power is mainly associated with system bus voltage magnitudes. Hence power system controllers can generally be categorized into the following: a) Active power and frequency controllers and b) Reactive power and voltage controllers.

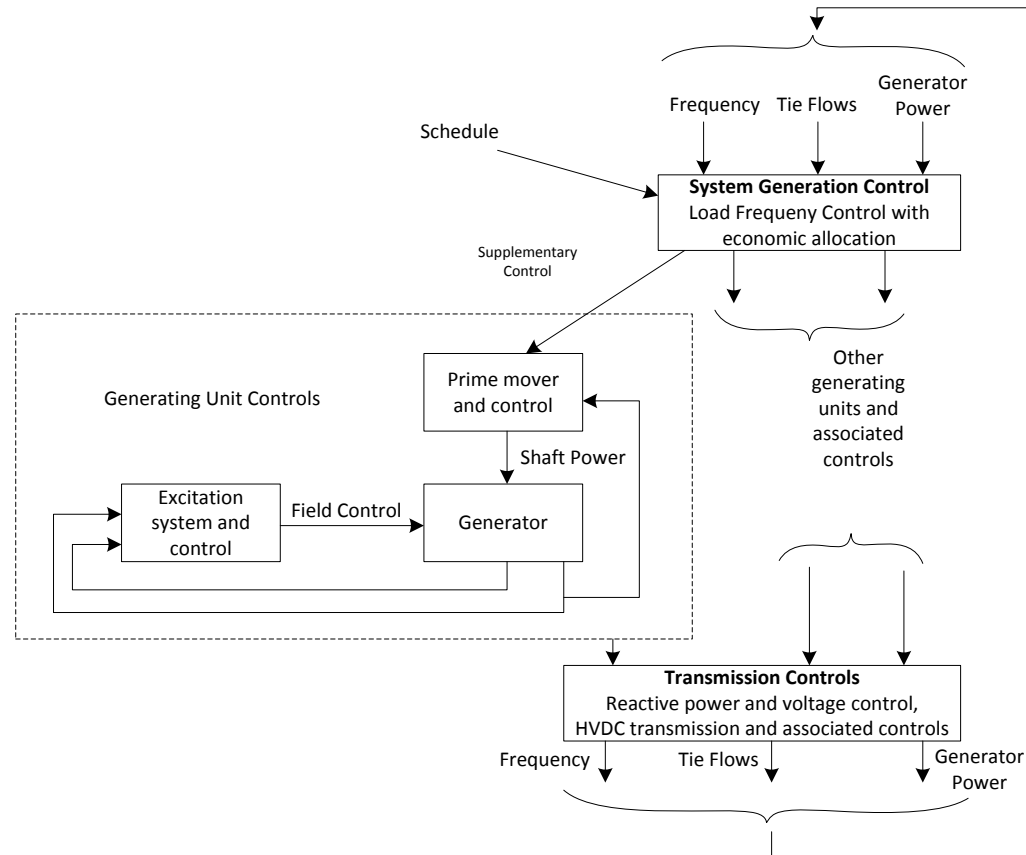


Figure 2.1: Schematic Diagram Illustrating Different Levels of Power System Control.

Generating unit controls are engaged in two stages :

1. At each individual generating unit level
2. At generation system level

Interconnected power system operation is enabled by the second one. The controls for the prime mover and excitation system are engaged to operate directly on a generating unit. Speed of the turbine is regulated by the prime mover controls, which governs the amount by which the valve/gate of turbine is to be opened, which affects the amount

of power output of the turbine [15]. Excitation control's main function is to control the voltage of generator and thus controlling the reactive power output. Excitation control system contributes to the stability of the system and helps to protect the system as well by ensuring that the machine is not exceeding beyond its operating limit.

System generation control is mainly focused on maintaining the generation level at a satisfactory level to meet the demand and loss as well as maintaining the system frequency level as close to its nominal value as possible. It is also an important function for this type of control to allocate generation according to scheduled generation dispatch [2] [3]. Transmission level controls include different types of devices for voltage and power control such as SVC, STATCOM, phase shifting transformers etc.

2.4 Active Power and Frequency Control

2.4.1 Response of a Generator to a Load Change

It was discussed earlier in Section 2.3 that active power control can be closely related to the control of frequency. To keep the system frequency close to its nominal value the active power generation and the load has to be maintained in balance. Frequency is a common factor throughout a system, as a result a change in active power demand at any point is reflected throughout the system by a frequency change from its nominal value.

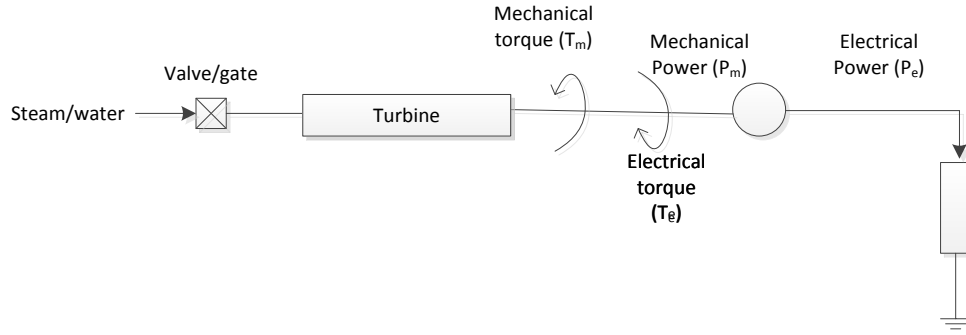


Figure 2.2: Simplified Diagram of an Isolated Load Supplied by a Generator.

In this system if there is an increase in load P_L , more electrical power will be demanded from the generator. Thus electrical torque output of the generator T_e will increase and result in deceleration of the machine if the mechanical torque T_m remains unchanged. Same way if the mechanical energy is in excess to that of the electrical energy which is being drawn out, then the excess mechanical energy will accelerate the machine and the speed of rotation will increase. Because of the synchronism between the generating units a change in speed will affect a change in system frequency.

This amount of change in frequency depends on the amount of power mismatch between load and generation and also the inertia from the rotating masses that is the turbine and generators. Inertia is a property of both turbine and generator that reflects the ability to store rotational kinetic energy [15] [16] [17]. It can be compared with the mass of a translational system. In a power system, there are usually several generating units connected together, so the frequency change rate depends on the total magnitude of the power mismatch and the total inertia of all the rotating mass.

The relationship between the frequency change, power mismatch and the system

inertia can be represented with the following block diagram:

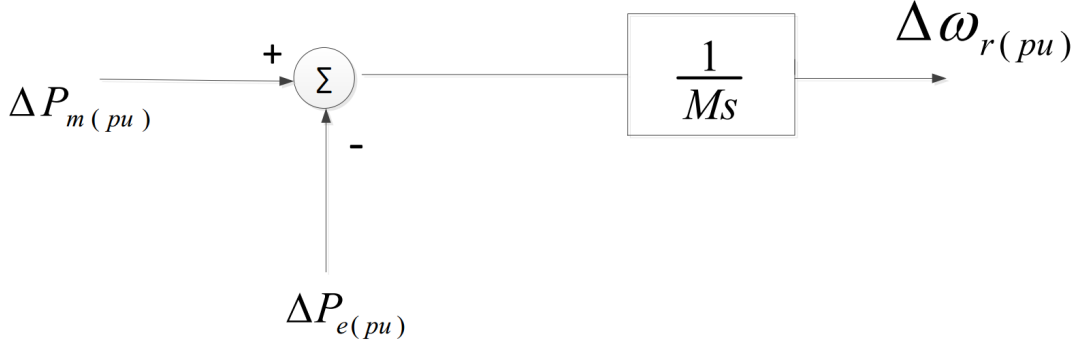


Figure 2.3: Block Diagram Showing the Relationship Between the Frequency, System Inertia and Power Mismatch.

Where, $M = 2H$; Here H is the inertia constant in $MW - Sec/MVA$

s : Laplace Operator

$\Delta P_{m(pu)}$: mechanical power deviation in per unit.

$\Delta P_{e(pu)}$: electrical power deviation in per unit.

$\Delta \omega_{r(pu)}$: rotor power deviation in per unit.

2.4.2 Load Response to Change in Frequency

Typically power system loads are made of a variety of devices. Some of them are resistive and some of them are inductive [15]. For resistive loads, they are independent of system frequency whereas the inductive loads are dependent on system frequency¹. Frequency dependent characteristic of a composite load may be approximated by a linear relationship as follows [18].

¹Frequency and speed are used in replacement of system frequency and generator rotor speed which has the same value when converted to per unit.

$$\Delta P_e = \Delta P_L + D\Delta\omega_r$$

where,

ΔP_L : non-frequency sensitive load in per unit

$D\Delta\omega_r$: frequency sensitive load in per unit

D : load damping constant

Where, D is expressed as.

$$D = \frac{\text{percentage change in load}}{1\% \text{ change in frequency}}$$

An example could be; if $D = 4$, then if frequency changes by 1%, the load active power would change by 4%.

Now including the effect of load damping in Figure 2.3 the transfer function block diagram can be represented as follows:

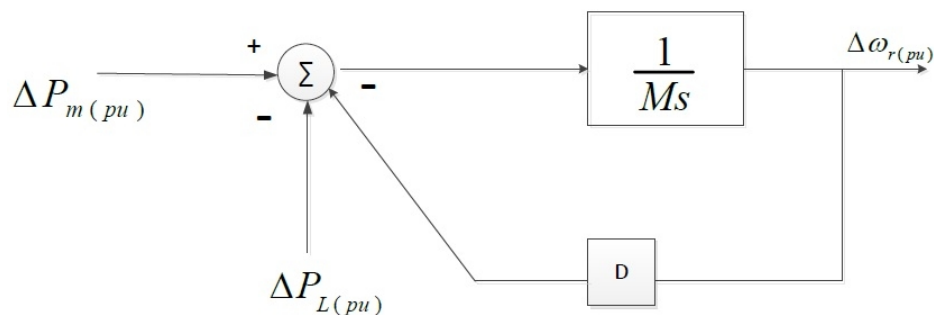


Figure 2.4: Block Diagram Including the Load Damping Effect.

The block diagram can be reduced and represented as Figure 2.5,

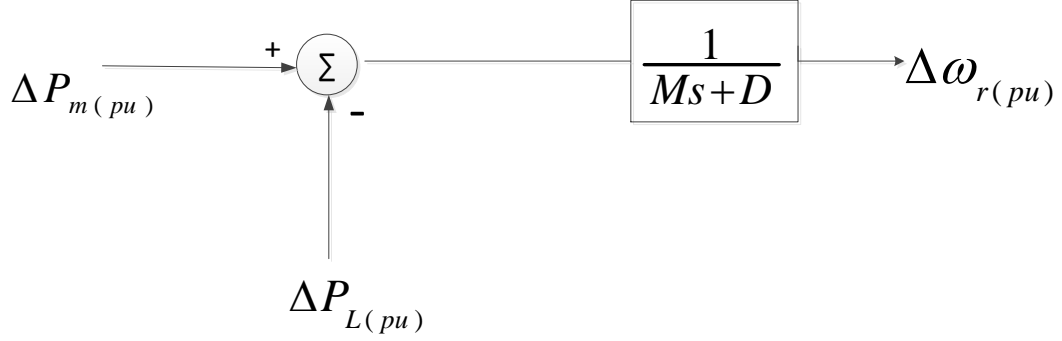


Figure 2.5: Reduced Block Diagram Including the Load Damping Effect.

Results obtained from a simulation of a model as shown in Figure 2.5 show that without any frequency control, a change in load will result in steady state frequency error. This error can be determined by the load damping constant (D). The speed deviation in steady state is such that the change in load is compensated by the variation in frequency dependent load.

2.4.3 Governor Speed Control

The basic function of a governor is to control the speed of the turbine thus controlling the frequency of the power system. The power output of the turbine is set by the speed reference which determines the amount of the opening or closing of the valve/gate [19] [20] [21].

When a difference occurs between the mechanical power and the electrical power balance, the speed deviates from the nominal value. The speed deviation is sensed by the speed transducer which produces a signal proportional to the change in speed.

The combination of the transducer output and the reference setting determine the net governor signal, which acts to adjust the input to turbine valve/gate to change the mechanical power output in such a way that the speed is set to a new steady state value [22] [17]. Figure 2.6 demonstrates the process in a block diagram.

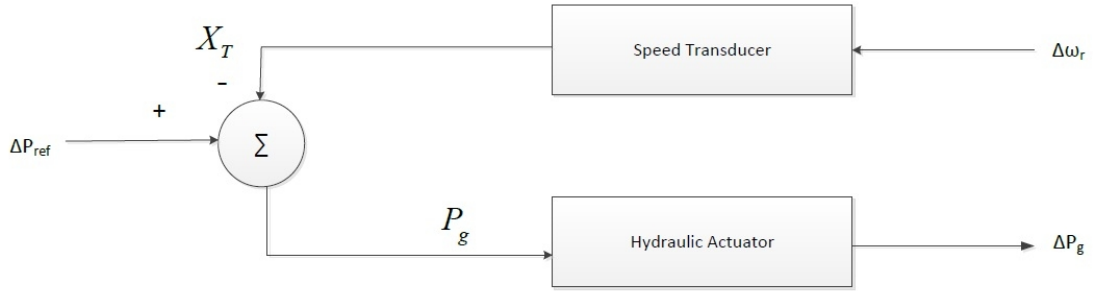


Figure 2.6: Representation of a Speed Governor in Block Diagram.

$\Delta\omega_r$ is the frequency error in Figure 2.6, ΔP_{ref} is the reference settings generator active power output, X_T is the output signal from the transducer and the P_g is the net governor signal. Hydraulic actuator controls the valve/gate opening depending on the error signal of $(P_{ref} - X_T)$. The transducer combined with the actuator is known as the speed governor. Figure 2.7 shows a generator combined with a turbine and speed governor supplying an isolated load.

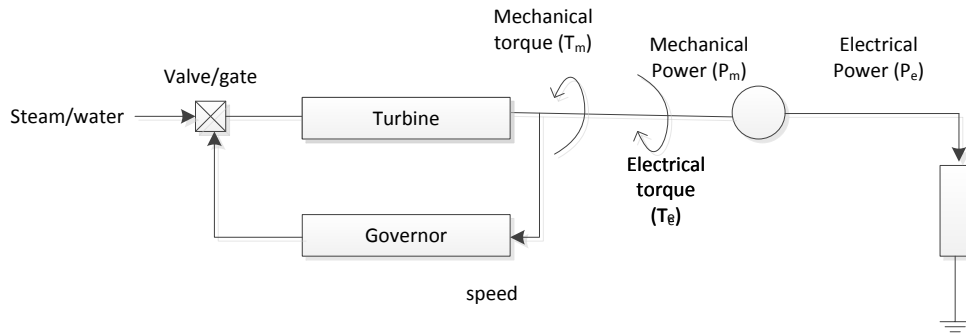


Figure 2.7: Generator With a Speed Governor Supplying an Isolated Load.

There are two types of governors: isochronous governor and speed droop governor [23]. If a single load is supplied by a single generator, isochronous governor is used. On the other hand, speed droop governor is used in case of two or more generators operating in parallel.

2.4.3.1 Isochronous Governors

Figure 2.8 illustrates an isochronous governor. In this figure the frequency error is amplified with a gain of K and integral of it is taken as a control signal (ΔY) which actuates the valve/gate to the turbine [14] [23].

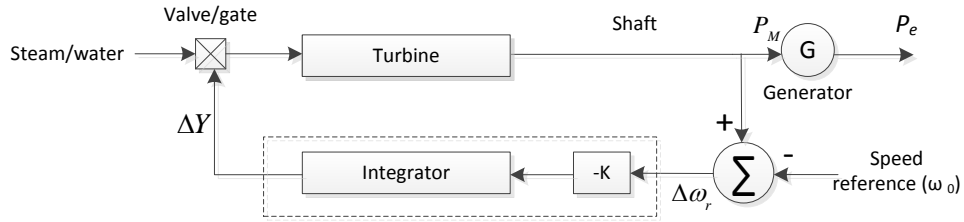


Figure 2.8: An Isochronous Governor Schematic Representation.

When a change in load occurs the frequency also deviates. The isochronous governor in this case will be in action and will adjust the turbine power so that frequency gets back to its reference value. This type of scheme is useful for a generator which is supplying an isolated load. However, the control system will get complicated if there are more than one generator operating in parallel and each having an isochronous governor. In that situation, each will try to control the system frequency to its own setting. This type of conflict between the governors could result in unexpected fluctuations in generator speed.

2.4.3.2 Speed Droop Governors

Speed droop governors use a methodology to share loads between two or more generators operating in parallel [23]. Figure 2-9 illustrates a block diagram of a speed droop governor [14]. In this case a feedback loop is added around the integrator to obtain the speed droop characteristic. The "load reference set point" could be adjusted to set any desired power output of the generator at a given speed [20]. In this type of scenario a servomotor can be used. As the servomotor can control the acceleration by changing the set point of the servomotor the expected level of dispatch can be scheduled at the nominal frequency.

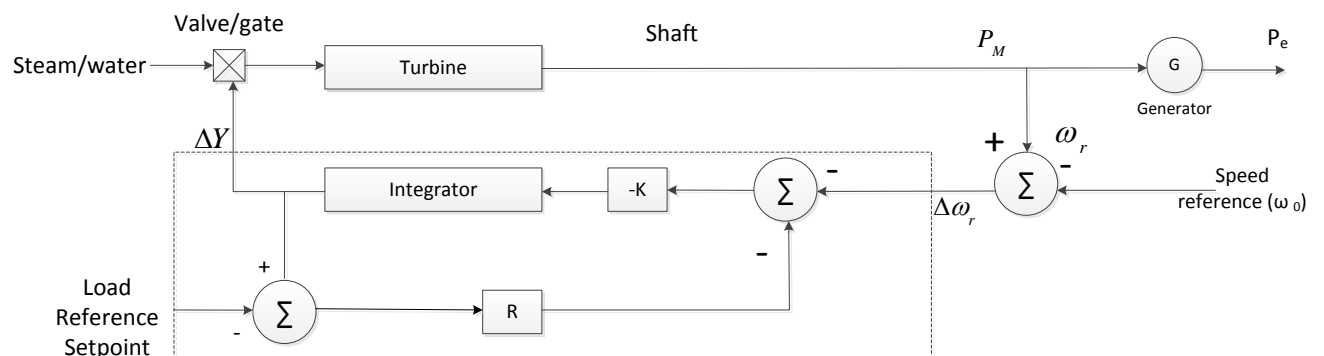


Figure 2.9: Speed Droop Governor Schematic Diagram.

This diagram in Figure 2.9 can be further reduced to obtain a schematic diagram as shown in figure 2.10

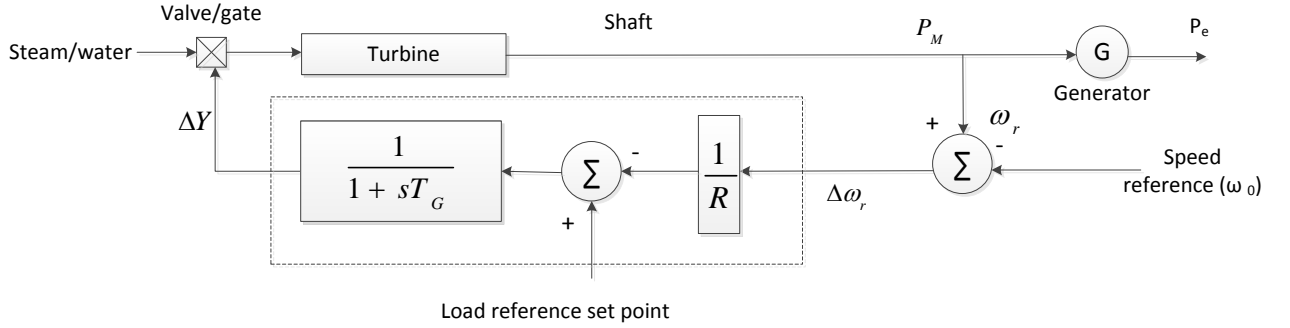


Figure 2.10: Speed Droop Governor With Reduced Governor Transfer Function.

The constant R is the speed regulation or the droop setting of the governor [22]. The amount of this is expressed in percentage, usually as:

$$R = \frac{\text{Percentage change in frequency or speed } (\Delta\omega)}{\text{Percentage change in power output } (\Delta P)}$$

An example of droop setting R could be: if a 50 MW generator has a droop setting of 2%, then for a 2% change in frequency, turbine power output will be changed by 50MW.

Droop characteristic provides a simpler way to share the generator output among multiple generating units [14]. When there are multiple generating units supplying the load, a change in generation output for a change in steady state frequency is determined by the droop characteristics of each of the governor that are connected and operated with the generating units.

2.4.4 Combined Speed Regulating Characteristic

The block diagram in Figure 2.11 is developed from the block diagram of Figure 2.5 that includes the load damping effect. This shows the system equivalent for load frequency

control.

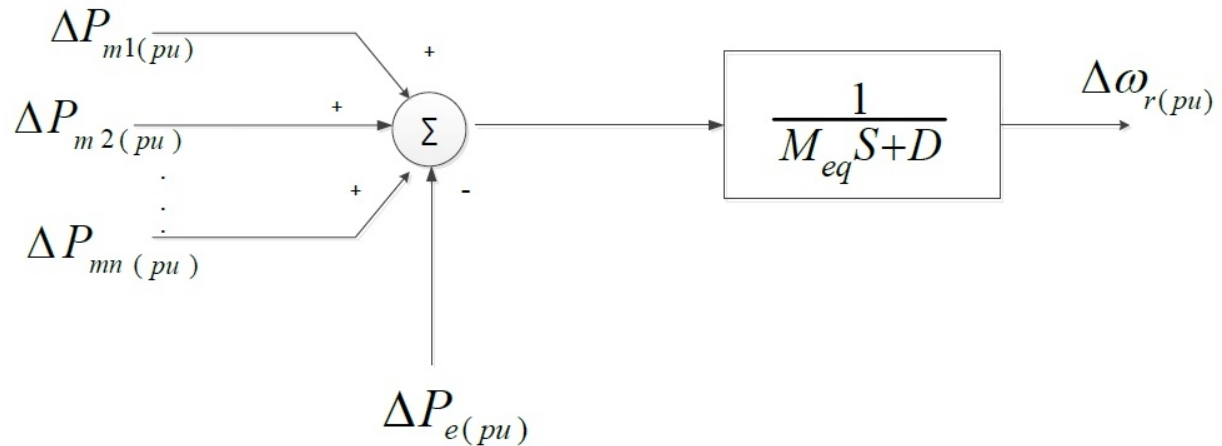


Figure 2.11: System Equivalent Representation with Transfer Function.

M_{eq} : sum of the inertia constants of all the generators. D : damping constant of the total system load.

For this system it can be showed that at steady state ,

$$(\Delta P_{m1} + \Delta P_{m2} + \dots + \Delta P_{mn}) - \Delta P_L = D\Delta\omega_{ss}$$

Where ω_{ss} represents the steady state frequency deviation.

As described in Section 2.4.3.2 the relationship between governor droop, generator speed and generator power output can be represented as,

$$\Delta P_m = \frac{\Delta\omega_{ss}}{R} \quad (2.1)$$

Using Equations 2.4.4), 2.1 it can be written as:

$$\Delta\omega_{ss}\left(\frac{1}{R_1} + \frac{1}{R_2} + \dots + \frac{1}{R_n}\right) - \Delta P_L = D\Delta\omega_{ss}$$

Where

$$\Delta\omega_{ss} = \frac{-\Delta P_L}{\left(\frac{1}{R_{eq}} + D\right)}$$

2.4.5 Frequency Control

In order to maintain the frequency at its target value, it is a requirement that the active power generation and consumption is controlled to maintain the balance between load and generation. A power system usually keeps a certain amount of active power, which is generally called frequency control reserve, for this type of control operation. Three sorts of frequency control are generally used to maintain the balance between generation and consumption of active power. They are primary frequency control, secondary frequency control and tertiary frequency control. A brief description of these three controls are explained in the following subsections.

2.4.5.1 Primary Frequency Control

In the case where two or more generators operating in parallel all have speed droop governors, they will react to a sudden change in load, independent of the load location. The speed droop characteristic of each generating unit will determine how each of the generator will react to this load change. This in turn will result in a steady state frequency error. This type of speed thus frequency control function by speed droop governors are referred to as "Primary Speed/ Frequency Control". This is an automatic control. It adjusts the active power generation and consumption to quickly restore the balance between the load and generation to restore the frequency to its targeted value. This type

of control engages almost all the generating units in the system. This type of frequency control is specifically designed to stabilize the frequency following large generation or load changes. Therefore for the stability of a power system primary frequency control is very important.

2.4.5.2 Secondary Frequency Control

When load change occur in the power system, frequency needs to be established to its targeted value by adjusting the load reference set point of the generator. This operation is done by the "Secondary frequency/ Speed control". Generators at the location of the imbalance will participate in this type of control as it is the responsibility of individual areas to maintain the load and generation balance. Output of the generator needs to be adjusted continuously to meet the continually changing load, so this requires an automated operation. This control function is known as "Automatic Generation Control" (AGC)[24]. AGC is not implemented in all the generating units. It depends on the capacity of the generating units and also accessibility to control. Some details of the AGC will be explained in a later section

2.4.5.3 Tertiary Frequency Control

Tertiary frequency control refers to manual changes to the output of the generating units. This control is used in the purpose of restoring the primary and secondary frequency control reserve. This control works as a back up to the secondary frequency control when it is unable to bring the frequency and interchange back to their target value.

2.4.6 Tie Line Bias Control

Tie line bias control is a widely applied and accepted mode of regulation to implement AGC in each area of a multi area interconnected system for most of the interconnected power system in North America [25] [26]. The functions of the tie line bias control can be divided into three sections as listed below [26],

1. It makes each area to absorb its own local load changes.
2. It helps to determine the response of an area to a remote load change.
3. It helps the control areas to implement its own frequency control responsibility.

Tie line bias control has to set the required generation for each area, to match the scheduled interchange, sum of area load and losses, and the area's share of support to the interconnection frequency [27] [28] in order to perform the above mentioned three functions. An area's share of support for interconnection frequency is determined by the area frequency bias characteristic adopted by that area. This will be described later in this section. To accomplish this control strategy a control signal called ACE is used by the Tie-line bias control. ACE is a control signal which is made up of the algebraic sum of a control area's two quantities. The first is the power mismatch which is the difference between the actual power flow and the scheduled power flow, and the second is the area's natural response to frequency deviation [25]. For a two area interconnected system of Area A and Area B, the control signal ACE could be written as,

$$ACE_A = \Delta P_{AB} - (10 * B_A * \Delta f)$$

$$ACE_B = \Delta P_{BA} - (10 * B_B * \Delta f)$$

Here the quantity B_A and B_B are the frequency bias factors for the respective areas. They are usually expressed as a negative value with the unit of MW/0.1 Hz. Frequency bias factor is a measure of frequency bias of the area. It represents the required change in generation for that area. ACE acts as an actuating signal which is applied to make the changes effective in the reference power set points. At steady state, ΔP_{AB} and Δf will be zero. Each control area works on to make the signal ACE to zero. The point at which all the control areas in an interconnection do this, the interconnection frequency can be achieved to its targeted value and all net power interchanges will be on its schedule [29].

If the frequency bias factor B is selected to be equal to the frequency-response characteristic, β of the area [26] [30] [9] then an overall satisfactory performance can be achieved. That is,

$$B_A = \beta_A = \frac{1}{R_A} + D_A$$

$$B_B = \beta_B = \frac{1}{R_B} + D_B$$

It is not a straight-forward task to obtain an accurate value for β , since it depends on the governor response capability of the generating units and also the frequency dependent loads which are constantly changing. Figure 2.12[14] illustrates a two-area interconnected power system with governors installed in the turbines and also the secondary speed control in selected generators of both areas.

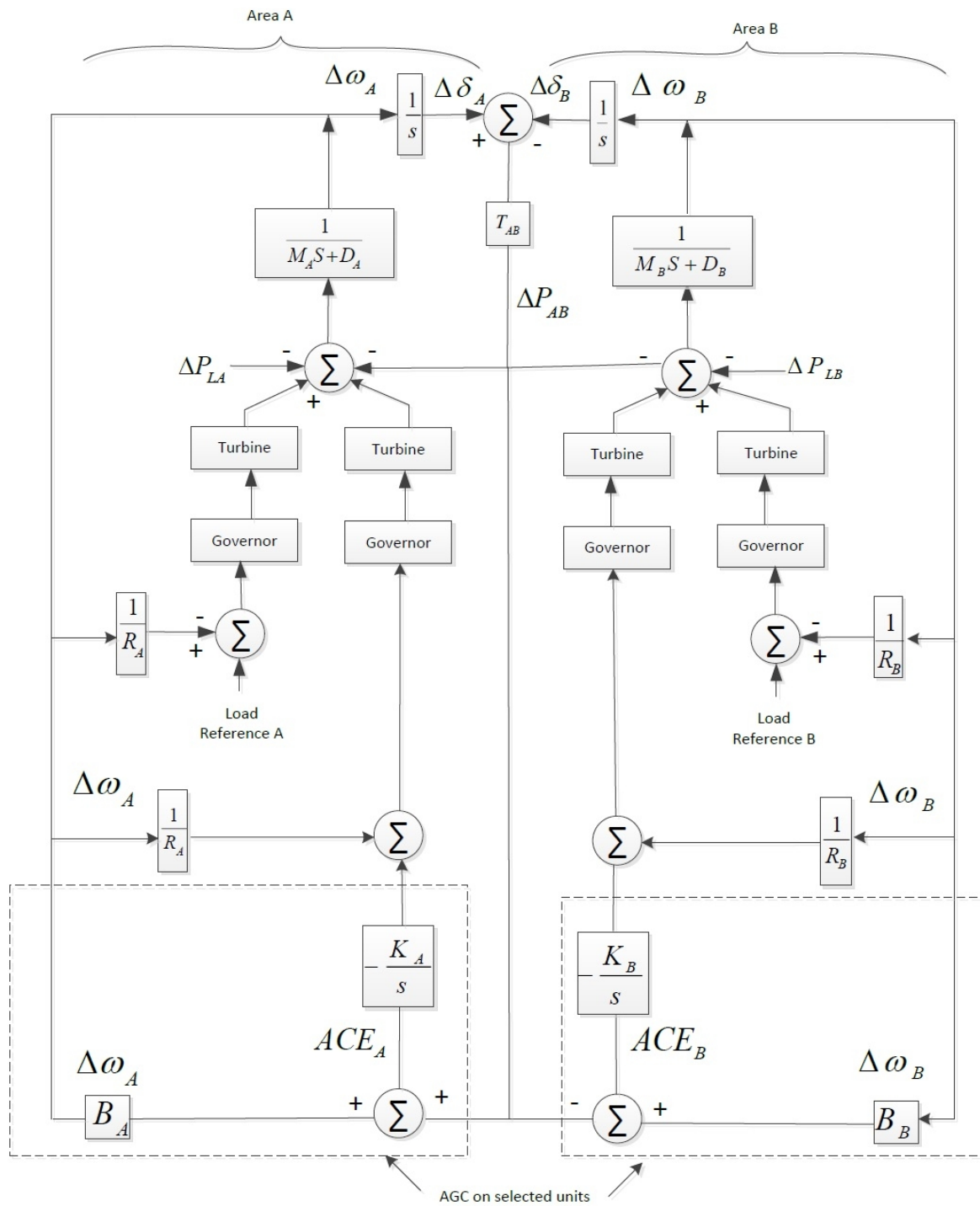


Figure 2.12: Block Diagram of Two Area Interconnected Power System With AGC.

2.5 Summary and Conclusions

An overview of a typical power system control functions is presented in this chapter. Load change response for generator producing active power is discussed. Load response to frequency change and various type of controls involved in a power system are also reviewed. Different levels of frequency controls and their importance are presented in this chapter. In order to analyze the NERC control performance indices, these literature background knowledge is important. The next chapter explains the NERC CPS1 index and relationship between its components.

Chapter 3

NERC Control Performance Standard

3.1 Introduction

NERC has been monitoring interconnected power system control area performance for many decades. CPS is a measurement with which all the interconnected control areas are evaluated. The requirement of reasonable control of the interconnection power flows and system frequency is the main reason for NERC to put on some standards for interconnected power systems. The CPS indices establish the statistical boundaries for ACE magnitudes, ensuring that steady-state frequency is statistically bounded around its target value. NERC demand that each Balancing Authority(BA) should achieve at least the minimum performance requirements of the CPS. Details about the CPS and its components are discussed in the later sections of this chapter.

3.2 Types of Control Performance Standards

The two main types of Control Performance Standard indices are CPS1 and CPS2. CPS1 is a measure of how well a system is reacting to restore its frequency to the target value and tie line interchange to its schedule. CPS2 measures that the average of ACE for each of the six ten minute periods in an hour must be within a predefined limit referred to as L_{10} and according to NERC BAL-001-0, it can not be less than 90% to be within compliance. In this research the main focus is on CPS1. Thus in the later sections discussions will be focused on CPS1 only.

3.3 Control Performance Standard 1

Frequency Profile of an interconnection shows the variation of frequency over time. This could indicate how well an area's generation is matching with the load. NERC has imposed a mathematical model for distributing control responsibility among control areas to achieve the scheduled frequency profile. A targeted frequency profile can be defined based on the frequency error averages. This can be calculated by taking the average of the frequency deviation from the target frequency value over a defined period of time. NERC CPS1 evaluates the performance of a control area under most normal operating conditions and defines whether the performance is satisfactory for a given amount of frequency error. Therefore it can clearly be stated that CPS1 is a frequency dependent parameter which imposes the following requirement on a control area of an interconnected power system [9]. For a given period of time the average of the clock one minute averages of the one tenth of ACE times corresponding clock one minute average value of that interconnections frequency error shall be less than or equal to a constant value [9]. In

the following equation the constant is stated to the right hand side as ε ,

$$AVG_{period} \left[\left(\frac{ACE_i}{-10 * B_i} \right)_{clock-one-minute-avg} * (\Delta f_i)_{clock-one-minute-avg} \right] \leq \varepsilon_1^2 \quad (3.1)$$

Where,

i: Designates the control area (e.g. i=1,2 for a two area system),

AVG: Average,

ACE: Area Control Error,

B: Frequency bias factor,

Δf : Clock-one-minute-average value of frequency error,

period: For control area evaluation it is one year or for the Resources Subcommittee review it is one month.

ε_1 : A constant derived from the targeted frequency bound.

ε_1 is the target root mean square (RMS) value of clock one minute average frequency error from a schedule based on frequency performance over a given year. This constant is calculated separately for each interconnection [31]. Within each interconnection for all of the control areas the constant is of same value.

Clock one minute average value of a quantity is calculated by averaging the samples of a parameter within a minute. At the end of each AGC cycle ACE and frequency error is recorded to calculate the one minute average values. In many North American systems the usual AGC cycle is 4 seconds [14]. Therefore in one minute there are 15 samples, hence clock one minute average value can be determined by averaging the 15 samples.

Results obtained from the calculation from Equation 3.3 helps to determine whether a

control area is in compliance with the CPS1 requirement or not. But it does not show the amount of compliance or non compliance. In order to express CPS1¹ as a percentage to quantify and determine the degree of compliance or non compliance the following equation is defined:

$$CPS1 = (2 - CF) * 100\% \quad (3.2)$$

The Compliance Factor (CF) is an important parameter in the calculation of CPS1. CF is usually a ratio of all the clock one minute compliance parameters accumulated over the period of time over which the CPS1 is calculated divided by the target frequency bound,

$$CF = \frac{CF_k}{\varepsilon_1^2} \quad (3.3)$$

k : It is the period of time over which the CPS1 is being calculated. For example $CF_{12-month-avg}$ is for compliance factors over a 12 month period.

Details about CF is described in Section 3.3.1.

If CPS1 results in equal or more than 100%, then according to NERC, the control area is satisfying the compliance. Area will be considered as fail to meet the compliance if CPS1 is under 100%.

¹CPS1 is used to refer the compliance percentage defined by Control Performance Standard 1

3.3.1 Calculation Process of Compliance Factor

ACE and Δf are two key components in calculating the Compliance Factor (CF). Clock-one-minute-average values of ACE and Δf for k th period of time are used to calculate the CF_k . Hourly, weekly, monthly and yearly averages of CF can be calculated using the ACE and Δf for the corresponding period. The steps for calculation are explained in the following subsections.

3.3.1.1 Calculation of Clock One Minute Averages

Clock-one-minute-average value can be defined as the average of a control area's any valid measured variable (*i.e.* ACE and Δf) for each sampling cycle (*i.e.* an AGC cycle) during a given clock-one-minute [9], which can be shown as,

$$\left(\frac{ACE}{-10B} \right)_{clock-one-minute-avg} = \frac{1}{-10B} * \left(\frac{\sum ACE}{n_{min}} \right)$$

Similarly,

$$(\Delta f)_{clock-one-minute-avg} = \left(\frac{\sum \Delta f}{n_{min}} \right)$$

Where, n_{min} is number of sampling cycles in clock-one-minute.

Hence, for a control area the CF can be represented in an equation as 3.4,

$$CF_{clock-one-minute-avg} = \left[\left(\frac{ACE}{-10 * B} \right)_{clock-one-minute-avg} * (\Delta f)_{clock-one-minute-avg} \right] \quad (3.4)$$

3.3.1.2 Hourly Average

Clock one minute average values of CF computed over an hour can be used to evaluate the respective hourly average of CF [9],

$$CF_{clock-one-hour-avg} = \left(\frac{\sum_{n_{min}} CF_{clock-one-minute}}{n_{hour}} \right)$$

Here, n_{hour} is the number of clock-one-minute samples in an hour.

By preserving the clock-one-hour-average values of CF for each of the 24 hours in a day and the number of clock-one-minute samples in each hour, the control area's clock k^{th} hour average for a given hour of a day (where $k=1,2,3,...,24$) can be calculated for a period of one month. *i.e.*,

$$CF_{clock-k^{th}-hour-avg-month} = \frac{\sum_{days-in-month} [(CF_{clock-k^{th}-hour-avg} * (n_{k^{th}hour}))]}{\sum_{days-in-month} (n_{k^{th}hour})}$$

Where, $n_{k^{th}hour}$ is the number of clock-one-minute samples in k^{th} clock-one-hour of a day.

3.3.1.3 Monthly Average

Clock-one-hour-average for each hour of all the days in a month and the total number of clock-one-minute samples for the corresponding clock-one-hour averages of all the days in the month can be calculated for a control area. Then by using these data the one-month-average value of CF can be obtained [9].*i.e.*,

$$CF_{one-month-avg} = \frac{\sum_{hours-in-day} [(CF_{clock-k^{th}-hour-avg-month} * (n_{k^{th}-hour-month}))]}{\sum_{hours-in-day} (n_{k^{th}-hour-month})}$$

Where, $n_{k^{th}-hour-month}$ is the number of clock-one-minute samples for the k^{th} clock-one-hour summed for all the days in a month.

3.3.1.4 Yearly Average

From the above discussion the 12-month-average value of CF can be written as follows [9],

$$CF_{12-month-avg} = \frac{\sum_{12-months} [(CF_{one-month-avg} * (n_{month}))]}{\sum_{12-months} (n_{month})}$$

Where, n_{month} is the number of clock-one-minute samples for all the days in a month. If any data is missing from the recording for all minutes/ hours/ day / months then the summations in the above formulas should be for the available data samples for minutes, hours, days and months respectively.

In order to make sure that the average ACE and Δf calculated for any one minute interval is a good reflection of that one minute interval, it is a necessity that at least 50% samples of both ACE and Δf are collected for that one minute interval. If there is a significant interval in the data recording due to technical difficulties such as loss of telemetering or computer equipment disruption resulting in the unavailability of at least 50% simultaneous sample pair of ACE and Δf , that one minute interval will be excluded [9] from the calculation process of CPS1.

The above discussion and calculation process is the pragmatic method of estimating CPS1. However for theoretical analysis that is going to be explained and used in this thesis, there are few assumptions which are as follows :

- (a) No fragmented data in any sampling cycle.

- (b) All the months in a year has the same number of days.

With respect to the above mentioned assumptions, the Equation for CF from (3.3) could be written as,

$$CF = \frac{1}{\varepsilon_1^2} \frac{\sum CF_{clock-one-minute}}{N} \quad (3.5)$$

Where N is the total number of all the clock-one-minute samples of CF during year of 12-month.

3.3.2 Data Reporting

Utilities conduct surveys each month for the CPS1 and CPS2 indices to analyze the level of compliance of each control area with the BAL-001-0. This provides a relative measure of each control area's level of performance according to NERC standards [9].

Each of the control area shall submit a completed copy of "CPS form 1"² which is also known as "NERC Control Performance Standard Survey-All interconnections" to NERC's Resources Subcommittee member representing the region, by the tenth working day of the month following the month being reported [9].

Using real data obtained from the power system and digital processing of ACE signal, all the control areas will complete the above mentioned form with the following necessary data and information,

- (a) Clock one hour average CF for each of the 24 hour period and total number of samples in each of the hourly average.

²this is a document implied by NERC, which contains necessary information related with CPS for that control area

- (b) Monthly CF
- (c) Rolling 12-month CF
- (d) CPS1 in percentage for rolling 12-month

3.4 Components of CPS1

According to Equation (3.2) CF and CPS1 are linearly related for an area of interest. This linear relationship can be illustrated in Figure A.1,

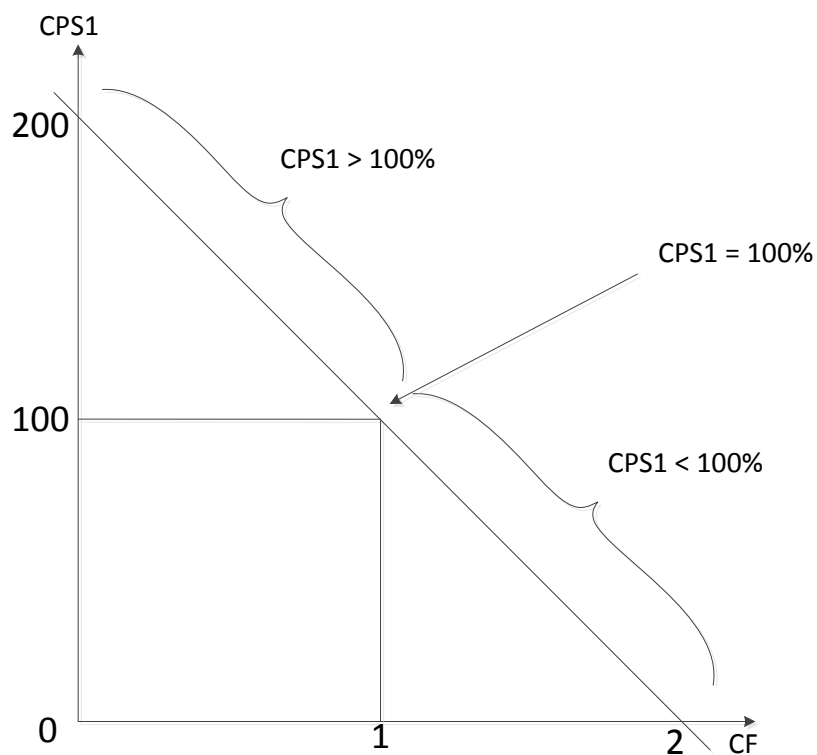


Figure 3.1: The relationship of CPS1 with CF.

Refer to Figure 3.1, when $\text{CPS1} \geq 100$, then $\text{CF} \leq 1$. Therefore, to be within compliance according to NERC, the CF value needs to be equal or less than 1.

A relationship between CF, Δf , ΔP can be obtained [10].

As illustrated in Section 2.4.6, ACE relates to Δf and ΔP as given in the following Equation 3.6,

$$ACE = \Delta P - (10 * B * \Delta f) \quad (3.6)$$

By substituting Equation (3.6) into Equation (3.4) the following can be obtained analytically,

$$CF_{clock-one-minute} = \left[\left(\frac{\Delta P - (10 * B * \Delta f)}{-10 * B} \right)_{clock-one-minute-avg} * (\Delta f)_{clock-one-minute-avg} \right]$$

$$CF_{clock-one-minute} = \frac{-1}{10B} [(\Delta P)_{clock-one-minute-avg} * (\Delta f)_{clock-one-minute-avg}] + \Delta f_{clock-one-minute-avg}^2 \quad (3.7)$$

Substituting 3.7 in 3.5,

$$CF = \frac{-1}{10B\varepsilon_1^2 N^2} \left[\sum (\Delta P)_{clock-one-minute-avg} * (\Delta f)_{clock-one-minute-avg} \right] + \frac{1}{\varepsilon_1^2 N^2} \left[\sum (\Delta f)_{clock-one-minute-avg} \right]^2 \quad (3.8)$$

Equation 3.8 can be written in a simple way:

$$CF = k_1 \sum (\Delta P_{1M} * \Delta f_{1M}) + k_2 \sum (\Delta f_{1M})^2 \quad (3.9)$$

Where ΔP_{1M} and Δf_{1M} stand for the clock-one-minute average value of tie line power deviation and clock-one-minute average value of frequency deviation respectively. In Equation 3.9 both k_1 and k_2 are two positive constants as following:

$$k_1 = \left(\frac{-1}{10B\varepsilon_1^2 N^2} \right) \text{ and } k_2 = \left(\frac{1}{\varepsilon_1^2 N^2} \right) \quad (3.10)$$

In order to relate an average power system behavior with CF, Equation 3.9 could be analyzed. This objective can be executed by considering different ranges of values for $\sum(\Delta P_{1M} * \Delta f_{1M})$ and $\sum(\Delta f_{1M})^2$.

For a control area in an interconnected power system if $\sum(\Delta P_{1M} * \Delta f_{1M})$ is positive that is an indication that the area is receiving help. On the other hand, if $\sum(\Delta P_{1M} * \Delta f_{1M})$ is negative, it indicates that the area is providing help. The process can be illustrated in the Figure 3.2[11].

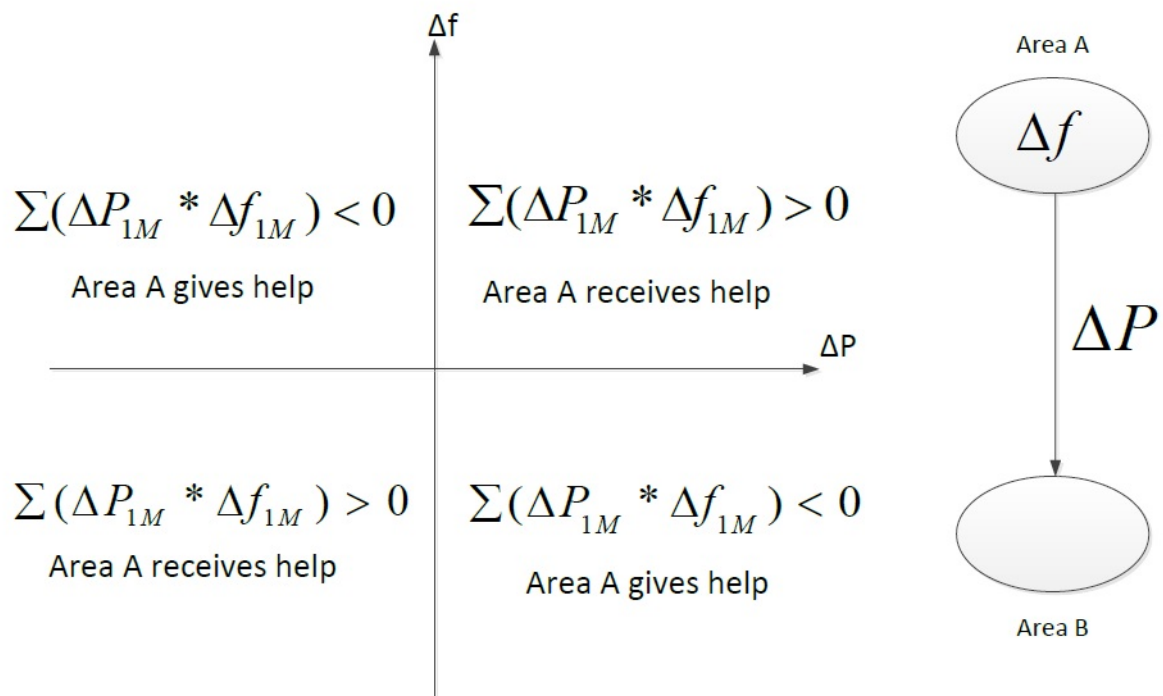


Figure 3.2: $\sum(\Delta P_{1M} * \Delta f_{1M})$ in different quadrants

Hence the sign of the first term of Equation 3.9 *i.e.* $k_1 \sum(\Delta P_{1M} * \Delta f_{1M})$ determines whether an area is receiving assistance from or is providing assistance to the interconnected system. If Δf_{1M} is equal to the target bound then the value of the second term of 3.9 which is $\sum(\Delta f_{1M})^2$ is unity. If the value is less than unity then it means the frequency control is in a tighter range than target bound and a value greater than 1.0 means the other way.

Various types of conditions arising from all possible values of the first and second terms of Equation 3.9 are tabulated in Table 3.1[10]. It also contains the range of values for CF and CPS1 for those combinations mentioned in the table.

Table 3.1: Range of CF and CPS1

$k_2 \sum(\Delta f_{1M})^2$	$k_1 \sum(\Delta P_{1M} * \Delta f_{1M})$	CF	CPS1(%)
< 1	> 0	$0 < CF < \infty$	$-\infty < CPS1 < 200$
	= 0	$0 < CF < 1$	$100 < CPS1 < 200$
	< 0	$-\infty < CF < 1$	$100 < CPS1 < \infty$
= 1	> 0	$1 < CF < \infty$	$-\infty < CPS1 < 100$
	= 0	= 1	=100
	< 0	$-\infty < CF < 1$	$100 < CPS1 < \infty$
> 1	> 0	$1 < CF < \infty$	$-\infty < CPS1 < 100$
	= 0	$1 < CF < \infty$	$-\infty < CPS1 < 100$
	< 0	$-\infty < CF < \infty$	$-\infty < CPS1 < \infty$

Theoretically CPS1 value could vary between $-\infty$ to $+\infty$, practical power system typically has CPS1 value ranging from usually 0 to 200. So the values $-\infty$ and $+\infty$ in Table 3.1 can be replaced with 0 and 200 respectively.

As mentioned in the table there are nine possible range of CPS1 that can occur. These could be further reduced to five possibilities by combining some of them under four possible ranges of CPS1 as shown in Table 3.2[10]. In Table 3.2 "Frequency Error" and "Type of support to the adjacent area" refer to the behavior of $\sum(\Delta f_{1M})^2$ and $\sum(\Delta P_{1M} * \Delta f_{1M})$, respectively.

Some conclusions can be drawn from Table 3.2[10]:

1. If a control area meets the necessary obligations ³ marginally then the CPS1 is equal to or slightly above 100% (i.e. the condition 1 in 3.2)

³Obligation refers to either frequency control or tie line power control

Table 3.2: CPS1 value in different conditions

Condition	Frequency Error	Nature of support to the adjacent area	CPS1
1	Equal to bound	Neutral	100
2	Equal to bound Out of bound Out of bound	Receives support Neutral Receives support	< 100
3	Within bound Within bound Equal to bound	Neutral Gives support Gives support	> 100
4	Within bound Out of bound	Receives support Gives support	< 100 or > 100

2. If a control area can meet only one of the obligations marginally or is unable to meet any of the obligations then its CPS1 value will be less than 100%, thus the area does not comply with the NERC BAL-001-0 standard requirements for CPS1 (Condition 2 in Table 3.2).
3. If a control area meets both of the obligations but one marginally, or if it meets both of the obligations marginally then CPS1 is always greater than 100%, and the respective control area complies with NERC standards (Condition 3 in Table 3.2).
4. If a control area can meet only one of the obligations and meet with marginal condition then that control area can have a CPS1 which is less than 100% or greater than 100%. Thus the area may or may not be complying with NERC standards (Condition 4 in Table 3.2).

Based on the above discussions a conclusion can be drawn that a control area will always be under compliance if it can meet both the obligations. On the other hand the area will not be able to meet the requirements of the BAL-001-0 standard, if both of the obligations are not met at the same time. However, if a control area

can meet only one obligation to determine if it is under compliance or not, it has to be decided based on the actual values of CF or CPS1.

3.5 Summary and Conclusions

NERC CPS indices were introduced in this chapter. The CPS1 and CPS2 indices help to evaluate the requirement of reasonable control of the interconnection power flows and system frequency for power systems. This chapter shows that the CPS indices establish statistical boundaries for ACE magnitudes. It has been shown that there is a close relationship between ΔP , Δf with CF. This relationship is useful to calculate CF with ΔP and Δf data. The next chapter describes the details of the System Identification and its application in the proposed methodologies.

Chapter 4

Application of System Identification Technique

4.1 Introduction

This chapter proposes two methods to estimate transfer function models using System Identification technique that can be used to estimate CPS1. The first method is applicable when a load-frequency time domain simulation model of an interconnected power system for estimation of CPS1 is available. The new method models an accurate approximate equivalent power system external to a system under consideration. The proposed approach uses existing dynamic simulation model of a power system to obtain necessary data to apply system identification technique. The second method is applicable when a time domain simulation model for the estimation of CPS1 is not available. This method uses System Identification to model two transfer functions to produce necessary data for the estimation of CPS1. The necessary up-to-date data for System Identification is obtained from available dynamic simulation model. This chapter lays the foundations for the above mentioned objectives by describing some basic theory of System Identification

and the use of MATLAB System Identification toolbox. Each step of the proposed approach is explained using simulation results. A North American Electric Power Utility's simulation model is used as an example to demonstrate the applicability of the proposed method. The contents of this chapter are as follows:

1. Basic introduction of System Identification.
2. Application of System Identification to improve the external system model for time domain simulation.
3. Develop transfer function models using System Identification technique to obtain Δf and ΔP data for the estimation of CPS1.

4.2 System Identification

System Identification can be defined as the process of determining a model of a dynamic system using observed system input-output data. Using the input and output data of a system, a mathematical model can be developed to predict the behavior of the system for a different set of inputs. System identification method has application in various fields. System Identification technique typically involves designing an appropriate input signal, using experimental input and output data, determination of class of models, construction of error criterion function, and lastly determining a model through optimization that fits the data best [32], [33], [34].

In a power system related study a large number of system parameters need to be determined. Most of the parameters are known in advance, but some are not. Often the missing parameters can be accurately approximated using standard values, but that may not be realistic in all cases. In such a case, System Identification methods can be

used to adjust the inaccurate parameter values. The System Identification technique can be used not only to approximate system parameters but also to predict the behavior of the system to certain changes from the estimated models. Some basic theories of System Identification is provided in Appendix A.

4.2.1 Classification of the System Identification

The System Identification problem can be classified in the following two categories [35]:

1. The complete identification: In this type of identification problem, the basic properties of the system (such as whether the system is linear or non linear, with or without memory etc.) are not known. This type of problem is extremely difficult to solve. Some assumptions need to be made before starting any solution attempt. This is also known as black box type problem.
2. Partial identification: In this type, some basic information is assumed to be known (such as bandwidth, linearity etc.) However, the specific order of the dynamic system or the values of the associated coefficients may not be known. This kind of problem can be called grey box problem; which is easier to solve as compared with black box type problem.

In this research, the type of problem is a grey box type problem. The step by step process that is followed to obtain the desired results is described in the later sections.

4.2.2 System Identification Procedure

The unknown parameters can be determined accurately in a system model equation where the measurements of input-output data are available [36]. There can be inaccuracies in a model equation; the system itself can also contain disturbances. Therefore, the System Identification is a statistical-estimation problem and a mathematical model is to be constructed to fit the observation data with or without noise.

The general procedure to carry out System Identification can be briefly described as follows:

1. A class of mathematical models has to be specified and parameterized that represents the system to be identified.
2. An appropriately chosen test signal can be applied to the system and the input/output data is recorded. If the system is in continuous operation and a test signal is not permitted, then normal operation data can be used for identification.
3. Performing of the parameter identification to select the model in the specified class that best fits the statistical data.
4. Performing a validation test to check if the model is chosen adequately to reflect and represent the system with respect to the identification objectives.
5. End the above procedure if it passes the validation test: otherwise another class of models must be selected and Steps 2 through 4 is performed until the model is validated to its desired level.

Use of the general procedure to identify transfer function models for a power system is one of the major contributions of this thesis. A flow chart for the transfer function identification process is provided in Figure 4.1

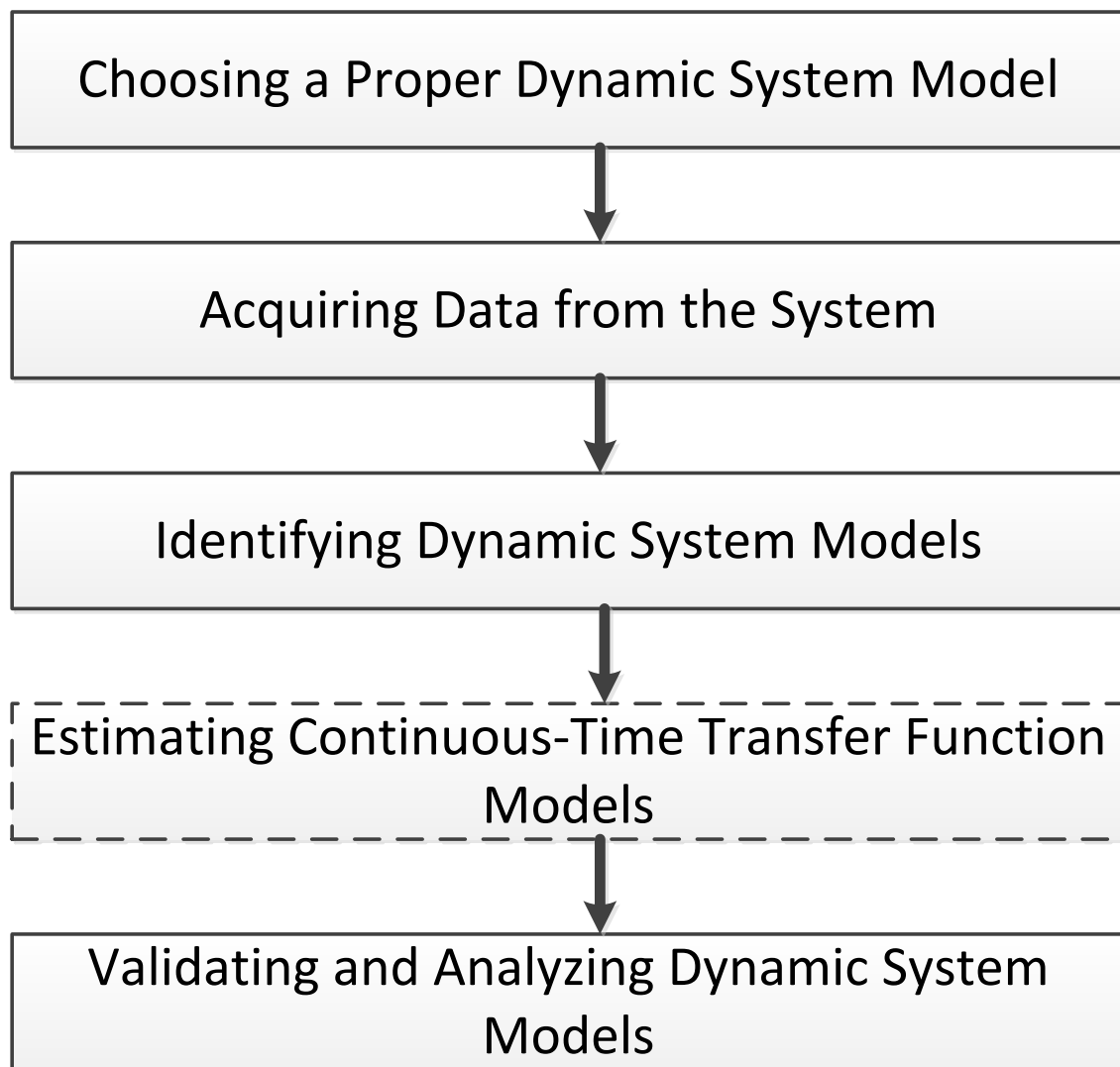


Figure 4.1: System Identification Procedure Flow Chart.

In this research the procedure as shown in Figure 4.1 has been followed. In the fourth step only transfer function model identification technique is mentioned. The reason is

that in this research transfer function models are estimated and have been used to serve the necessary purpose.

A number of possible representations can be selected for a system, including models characterized in the frequency domain or the time domain, in continuous time or discrete time. The choice depends on identification objectives and its related input/output data.

4.3 Estimation of Transfer Function Models Using MATLAB System Identification Toolbox

The MATLAB software by Mathworks has a System Identification Toolbox which is used in this research project. The toolbox is rich with its functions and useful for different kind of model object identifications. In this section, the general use of the toolbox for different model object identifications and the detail process of transfer function identification are discussed. A view of the System Identification Toolbox is illustrated in Figure 4.2

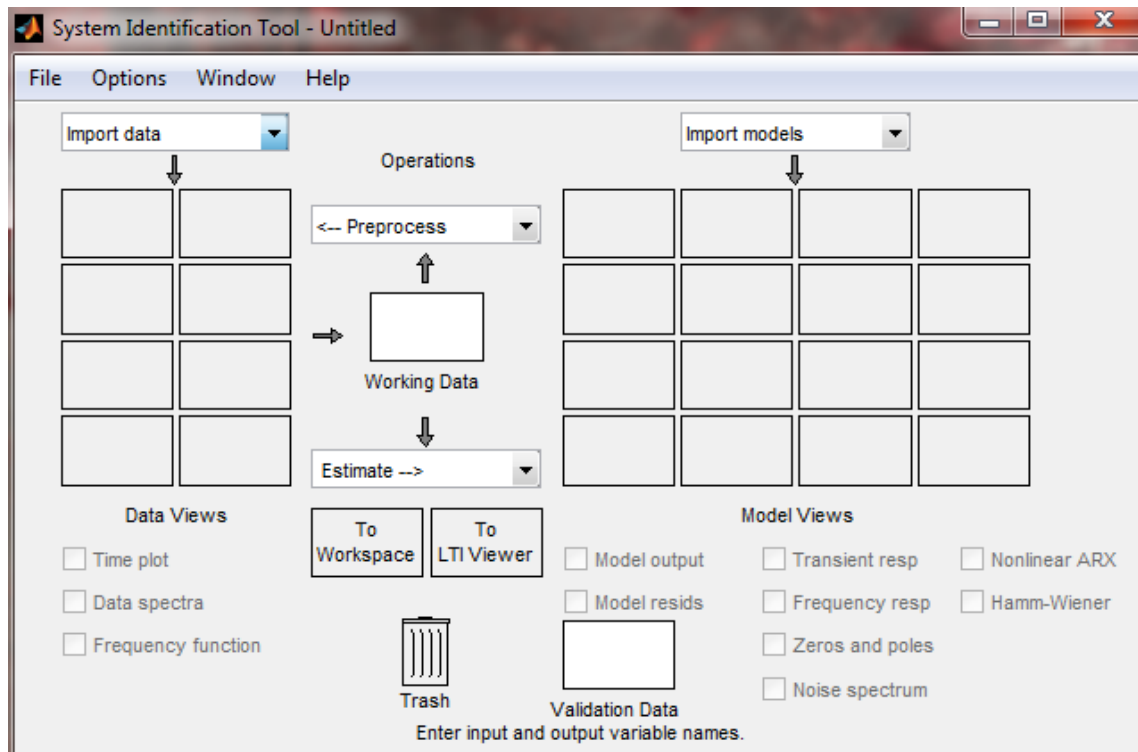


Figure 4.2: Interface of MATLAB System Identification Toolbox.

The Graphical User Interface has a simple and user friendly arrangement. There are options to import necessary data, pre-process the data, and then estimate models. There are also options for various types of plotting. Some of the features of MATLAB System Identification Toolbox that were used in the research described in this thesis are briefly described in the following sub sections.

4.3.1 Model Objects

In the MATLAB System Identification toolbox the linear systems are represented as model objects. *Model Objects* are specialized data containers that encapsulate model data and other attributes in a structured way [37]. Model objects allow to manipulation of linear systems as single entities instead of tracking multiple data vector matrices, or

cell arrays.

Model objects can represent different type of systems, such as, single-input, single-output(SISO) systems or multiple-input, multiple-output(MIMO) systems. Both continuous and discrete time linear time systems can be represented. The main families of model objects are as follows:

- **Numeric Models** - Basic representation of linear systems with fixed numerical coefficients. This type of family also includes identified models that have coefficients estimated with System Identification Toolbox Software.
- **Generalized Models** - Representation of systems that combine numeric coefficients with tunable or uncertain coefficients. Generalized models support tasks such as parameter studies or compensator tuning.

The data encapsulated in model object depends on the model type for which it is used. Some examples are as follows:

- Transfer function models store the numerator and denominator coefficients.
- PID controller models store the proportional, integral, and derivative gains.

4.3.1.1 Available Linear Transfer Function Model

A linear model is often sufficient and can accurately describe the system dynamics and in most cases it is recommended to try to fit linear models initially. In this case, the assumed system behavior is linear; thus only linear model will be followed. Available linear model structures include transfer function model, which is used in this research.

The available transfer function structure can be used to represent a transfer function in the following way:

$$y = \frac{num}{den}u + e$$

Here, y is output, u is input and e is noise(or error). num and den are numerator and denominator respectively.

More about the transfer function identification using the toolbox is described in the later sections.

4.3.1.2 Model Properties

The way a model object stores information is defined by the *properties* of the corresponding model class. Each model object has properties for storing information that are relevant only to that specific model type. In general, all the model objects have properties that can be described in the following categories:

- Input and output channel names, such as Input Name and Output Name
- Model sampling interval or time step, such as T_s
- Time or frequency units
- Model order and mathematical structure
- Properties that store estimation results such as report
- User comments, such as notes by the user

4.3.2 Input/Output Data

System Identification Toolbox software supports different type of data for estimation of linear models. This includes both time- and frequency- domain data.

The data can be of various types:

1. Single or multiple inputs and outputs.
2. Real or complex numbers.
3. Time or frequency domain data.

This research focuses on SISO systems. The data used is time domain data. The time-domain data should be sampled at discrete and uniformly spaced time instants to obtain an input sequence as showed in Equation 4.1,

$$u = u(T), u(2T), \dots, u(NT) \quad (4.1)$$

and a corresponding output sequence as showed in Equation 4.2,

$$y = y(T), y(2T), \dots, y(NT) \quad (4.2)$$

Where $u(t)$ and $y(t)$ are the values of the input and output signals at time t , respectively.

The toolbox is used in this research to model transfer functions which uses SISO time domain data obtained from a real power system simulation model.

4.3.2.1 Time-Domain Data Representation

Time-domain data can consist of one or more input variables $u(t)$ and one or more output variables $y(t)$, sampled as a function of time.

The time domain input/output data has to be organized in the format that is required for SISO systems. The sampled data values must be double column vectors: one is time instants and the other one is the corresponding data. To use the time domain data for identification, the sampling interval must be known. The actual sampling interval needs to be used if the data is uniformly sampled (which is the case in this research). Each data value is assigned with a time instant and a sampling interval.

4.3.2.2 Import Time-Domain Data into the GUI

Data can be imported from external data files or can also be manually created and then imported to the MATLAB work space. After importing the data to the work space in MATLAB the next step is to import them in the System Identification Toolbox GUI. It should be noted that the input and output data signals must have the same number of data samples.

To import data into the GUI:

1. The System Identification Toolbox is opened from the command window by typing "ident".
2. In the System Identification Tool window, using the time domain data option under import data menu the data is imported to the GUI.
3. The following options have to be mentioned while importing data:
 - **Input and output** - The MATLAB variable name has to be entered (column vector or matrix) or a MATLAB expression that represents the input and

output data should be selected. The expression must be evaluated to a column vector or matrix.

- **Data name** - A name can be entered for the data that is being used. This name appears in the toolbox window after importing the data.
- **Starting time** - For time plots, the initial time should be mentioned.
- **Sampling interval** - Actual sampling interval is entered in the identification process. The sampling interval is the time between successive data samples in the experimental data and it is the numerical time interval at which the data is sampled in any unit. For example, if the data is sampled at every 1 second then in the respective box '1' needs to be entered. The sampling interval is used during model estimation. In time-domain data, the sampling interval is used together with the start time to calculate the time instants of sampling.

4.3.3 Identifying Transfer Function Models

4.3.3.1 Definition of Transfer Function Models

Transfer function models are used to describe the relationship between the inputs and outputs of a system using ratio of polynomials [37]. The order of the transfer function model is equal to the order of the denominator polynomial of the transfer function. The roots of the denominator polynomials are referred to as the model *poles* and the roots of the numerator polynomials are called the model zeros.

The main parameters of a transfer function model are its poles, zeros. In continuous-time, transfer function model in the Laplace domain has the form:

$$Y(s) = \frac{num(s)}{den(s)}U(s) + E(s)$$

Where, $Y(s)$, $U(s)$, and $E(s)$ represent the Laplace transforms of the output, input, and noise, respectively. $num(s)$ is the numerator and $den(s)$ is the denominator polynomials that define the relationship between the input and the output.

4.3.3.2 Estimation of Transfer Function Models

At the beginning of the process as described in the earlier section the data is imported to the GUI. Then the next step would be to choose the Transfer Function Models option from the Estimate menu. Figure 4.3 shows the option to select the transfer function estimation inside the System Identification Toolbox GUI.

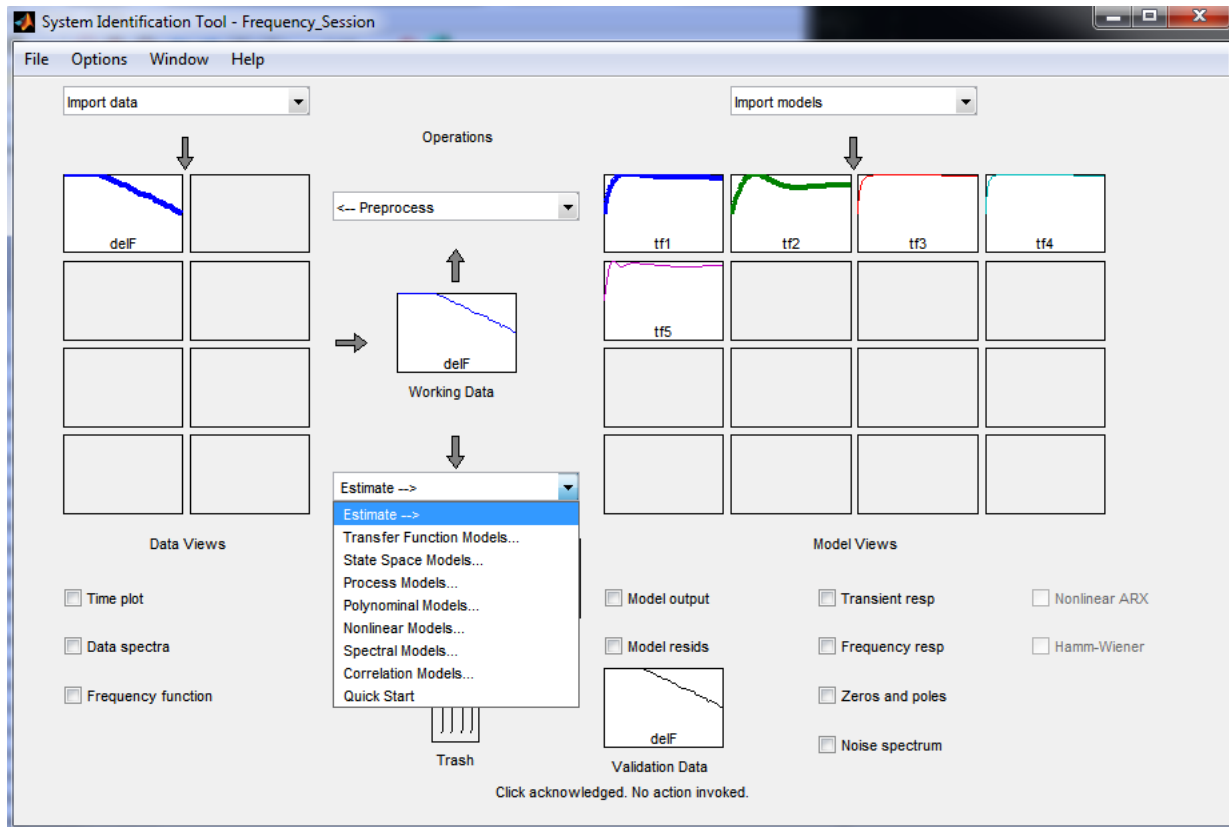


Figure 4.3: Transfer Function Identification Dialogue Box.

The number of poles and number of zeros of the transfer functions are specified as non negative integers. Figure 4.4 shows the respective options for selecting number of poles and zeros.

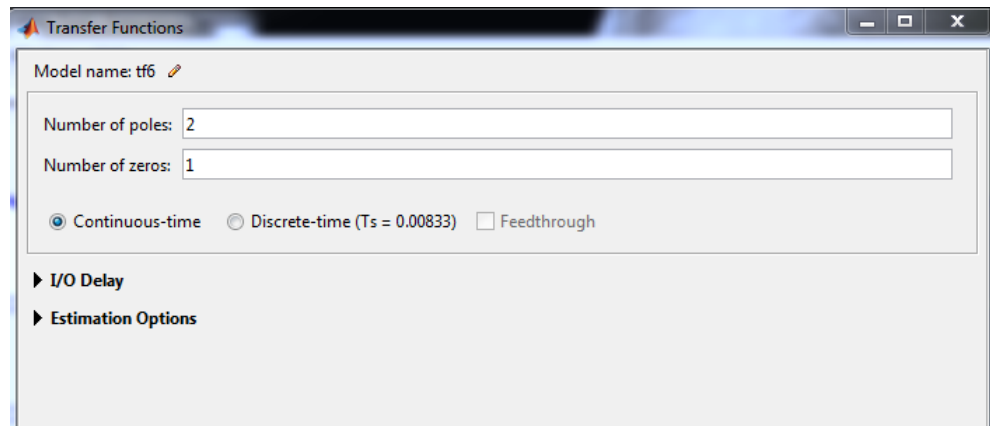


Figure 4.4: Selection of Number of Poles and Zeros for the Transfer Function Estimation.

For continuous time models, the number of zeros must be less than or equal to the number of poles, depending on the transfer functions that will be identified. Several combination of poles and zeroes can be chosen and corresponding transfer function model can be estimated to find the best match. The identified model can then be validated with a base signal which is usually the output signal that is used to figure out the best and most practical option for a particular purpose.

4.3.3.3 Model Output Validation

The output of the identified transfer function model can be validated by comparing it with the output data that is used to estimate the model. This is achieved by feeding the input data to the identified model. Two types of data sets are designated for plots that compare model response to measured response and perform analysis. One is for the estimation of the models (estimation data), and the other is for validation of the models (validation data). The Same data can be used for estimating and validating the model.

The model output plot can be created for linear models in the System Identification

Tool GUI. Using this operation, the output from the estimated model can be plotted and compared with the estimation data output signal. A number of estimated model outputs can be plotted in one graph and can be compared. The simulated or predicted model output can be plotted together with the measured validation data. The percentage of the output variations that is reproduced (Best Fit) by the model is displayed at the side of the plot. This number can be both positive and negative real numbers. A higher positive number means a better model. This fitting is computed by the following equation:

$$BestFit = \left(1 - \frac{|y - \hat{y}|}{|y - \bar{y}|} \right) * 100$$

In this equation y is the measured output, \hat{y} is the simulated or predicted model output, and \bar{y} is the mean of y . 100% corresponds to an exact match, that is a perfect fit. On the other hand 0% indicates that the fit is no better than guessing the output to be a constant ($\hat{y} = \bar{y}$). If a best fit is negative, then it is even worse than 0%. The following situations can be the unfavorable results of this type of estimation:

- The algorithm for estimation has failed to converge.
- Model estimation was not done by minimizing $|y - \hat{y}|$. Best fit can be negative in a situation when 1 step ahead prediction is minimized during the estimation process.
- The validation data was not pre-processed in a similar way as the estimation data set.

4.4 Modeling an Enhanced External System for a Time Domain Simulation of an Interconnected Power System

4.4.1 Proposed Methodology

The first method that is proposed in this research is to model a transfer function using System Identification technique. This transfer function model accurately represents the power system external to a system under consideration.

For modeling an appropriate transfer function to represent the external system, the required data is frequency deviation (Δf) and tie line power deviation (ΔP). To obtain the necessary data, an existing dynamic simulation model of a power system under consideration is used. The data should contain enough details, such as the obtained data should contain information when the system is in normal operation as well as when a disturbance occurs to the system. For the data collection purpose from the detailed dynamic simulation model, the following steps can be followed:

- Initialize the simulation system
- Provide a disturbance to the system: in this case a change in load
- Run the simulation until it settles down after the initial effect of disturbance
- Record necessary data

A change in load to the system under consideration affects both Δf and ΔP . Δf is collected at the border bus between the two areas under consideration. ΔP is collected

between the transmissions lines connecting the two areas under consideration. When a set of data is collected, it is used to model transfer functions using the System Identification technique. The process of modeling transfer functions using System Identification is followed step by step as mentioned in Section 4.3.3.

An example of this method is presented in the next section. A practical simulation model of a North American Electric Power Utility is used. The method is applied and successfully validated in a time domain simulation model of Manitoba Hydro, that was developed using PSCAD/EMTDC simulation software package.

4.4.2 Load Frequency Simulation Model

A time domain simulation model of Manitoba Hydro in PSCAD is used in this research to validate the proposed method of modeling an external system. After developing the transfer function model of an external system the CPS1 is estimated using the method from [10]. The original time domain simulation model of Manitoba Hydro is proposed in [13]. This model represents Manitoba Hydro and its Southern external system. The basic structure of the load frequency model is shown in Figure 4.5:

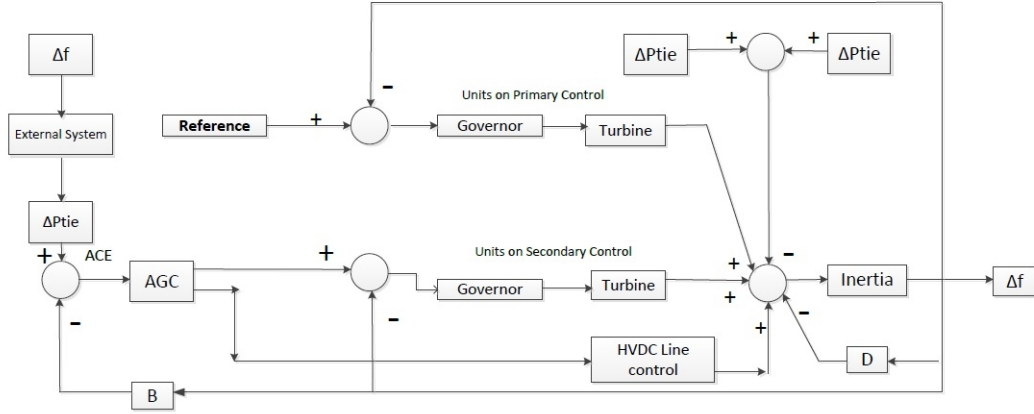


Figure 4.5: Manitoba Hydro Load-Frequency Model.

The power system of Manitoba Hydro is modeled as a control system with equivalent representation of the turbine and governor dynamics. The inertia of the system is modeled as a single equivalent inertia [13]. The power system external to Manitoba Hydro is modeled as a single equivalent. This model is designed in the PSCAD/EMTDC electromagnetic transient simulation program using control blocks [13]. The generating units of Manitoba Hydro are separated in two different categories. The purpose is to model their governor and turbine responses. A single governor-turbine model is modeled for the units equipped with secondary frequency control (Automatic Generation Control or AGC). A negative load representation is modeled and added to the system for the High Voltage DC (HVDC) converters. This model enables the HVDC converters to be on AGC duty. As a result it is possible for the AGC to generate signals to both the generators on AGC and the HVDC converters. In Figure 4.5 the parameter D is the load damping. This exhibits the frequency dependency of the load [38]. A change in load in the Manitoba Hydro side will cause a frequency deviation. Whenever there is a frequency change deviated from its nominal value it results in a deviation of tie line power flow to the adjacent area. The transmission line connecting the external system to Manitoba

Hydro system is modeled using an integrator. The gain of the integrator represents the synchronizing coefficient of the line. There are switches provided to the model which can be used to operate the control modes of the HVDC bi-poles and the units on AGC duty. Generating units can also be controlled and switched on/off during the simulation. The input to the model is a measured set of system load variation, and frequency and tie line power deviation are simulated. Per unit values were used throughout the model. The base value for the power is used as the total generating MW unit. Frequency base is used as 60 Hz.

The external system for this simulation model was initially modeled in [13]. Later it was modified in [38] which is shown in the following figure:

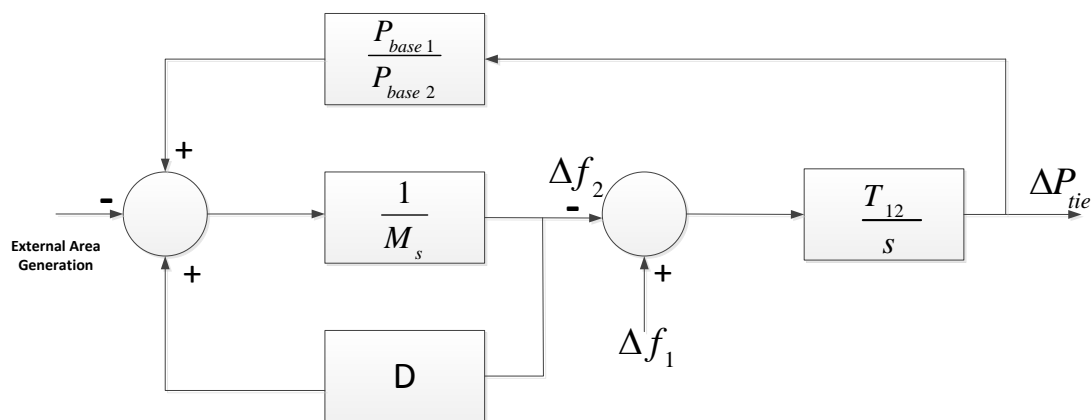


Figure 4.6: Model of the External System

The above model has inertia ($M = 10$), damping ($D = 0.25$) and tie line synchronization coefficient ($T_{12} = 1.538$). This model does not have any controllers modeled in it. Net effect of damping is represented by the damping D . Part of this external system model was built with trial and error to obtain a close match of simulated and recorded MH system frequency. Thus this model is not able to produce accurate results in a wide

variety of situations.

The purpose of applying the proposed method which is described in Section 4.4.1 are as follows:

- To enable the assessment of frequency control performance indices more accurately using data generated from time domain simulations.
- To have an enhanced load-frequency model which can be used for various types of studies. For example, studies related with integrating wind generation to the current system, studies related with optimization of regulating reserve management etc.

4.4.3 External System Modeling For a Practical Power System

In the time domain simulation model described in Section 4.4.2, the input to the external system is frequency deviation and the output from the external system is tie line power deviation. To develop a more accurate external system model for time domain simulation, System Identification technique is used. In this regard the input and output signal used in System Identification process is frequency deviation and tie line power deviation respectively. For this purpose up-to-date data of the existing PSS/E dynamic simulation model developed and updated by Mid West Reliability Organization (MRO) is used. This simulation model is 2011 series MRO stability package. This PSS/E dynamic simulation case has detailed models of all the control areas of the Eastern Interconnection and is extensively used in various studies of Manitoba Hydro planning and operational purposes. For this reason it is considered as a reliable source to collect necessary data.

To apply the System Identification technique frequency deviation data is obtained from the Manitoba side border buses connected to USA. The tie line power deviation is obtained from the power exchange between the four tie lines connecting Manitoba and US systems.

In the PSS/E simulation, after initialization, a load change is applied to a large industrial load at the Manitoba side. It is observed that the system settles down after the initial effect of load change within 3 to 4 seconds. Three step load changes were provided. Each load change is provided with a duration of 10 seconds. The simulation is run for 30.1 seconds. Frequency deviation and tie line power deviation data were recorded from the simulation. Using collected data, system identification technique is applied to estimate a transfer function as described in earlier sections. The estimated transfer function model has a fit to estimation rate of more than 82% with the original data. MATLAB System Identification Toolbox [37] is used to carry out the System Identification process. The details of the toolbox and how to use them are explained in Section 4.3.

If frequency deviation data is provided as input to the modeled transfer function, it can produce output as corresponding tie line power deviation. The identified transfer function model of external system is a second order 2 poles and 2 zeros transfer function as follows:

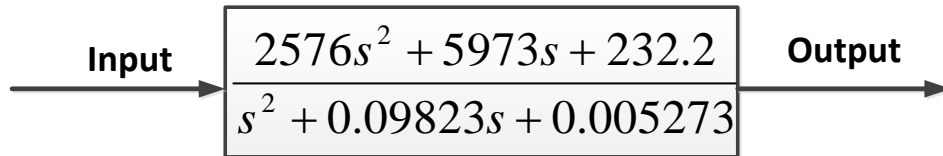


Figure 4.7: External System Modeled Using the Proposed Methodology

The transfer function shown in Figure 4.7 is an enhanced external system model for the time domain simulation model described in Section 4.4.2. Using this approach an appropriate external system model can be developed for different scenarios. This approach can be applied for any other power system in a situation where an up-to-date dynamic simulation model is available to obtain necessary data for the application of System Identification.

In order to show that the proposed method is producing better results, the previous external system model and the external system modeled with the new approach is compared with each other in Section 4.4.4.

4.4.4 External System Model Testing and Observation

In this section, the previously used external system and the external system modeled with the proposed method is compared to show that the new method is able to produce more accurate results.

The input to the external system models is frequency deviation in Hertz, which was recorded and obtained from the Manitoba Hydro power system during a day in the month of May in 2006. The input is shown in Figure 4.8. This is an hour long data window. The tie line power deviation recorded from the system for the same time frame is as shown in Figure 4.9.

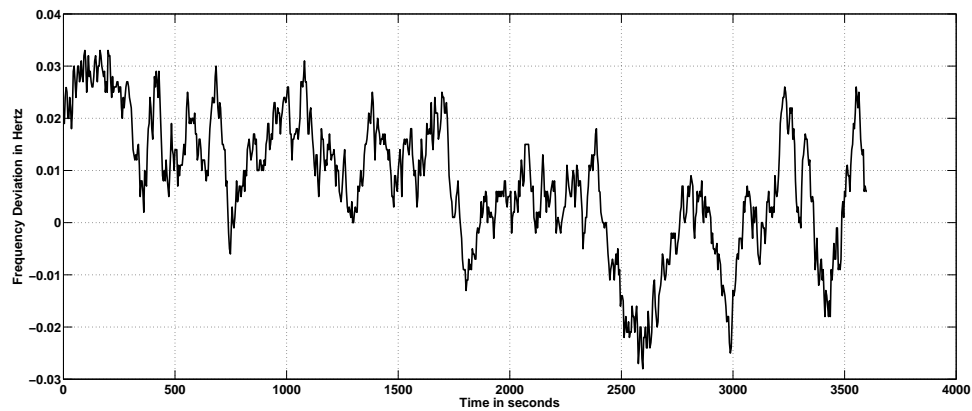


Figure 4.8: Measured Frequency Deviation in Per Unit.

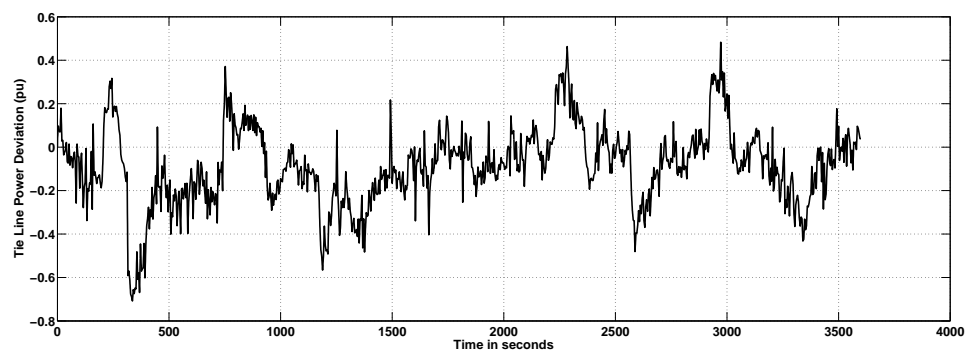


Figure 4.9: Measured Tie Line Power in Per Unit.

The frequency deviation shown in Figure 4.8 is applied to both of the external system models. The outputs obtained are presented, respectively in Figure 4.9 and Figure 4.10

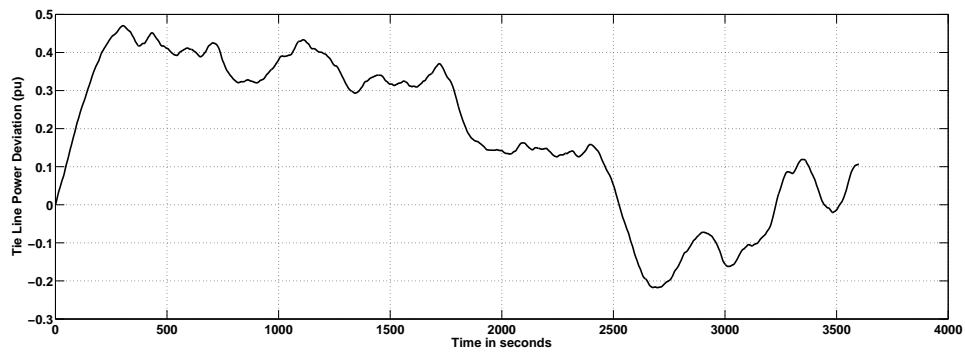


Figure 4.10: Tie Line Power Deviation in Per Unit (generated from the previous model).

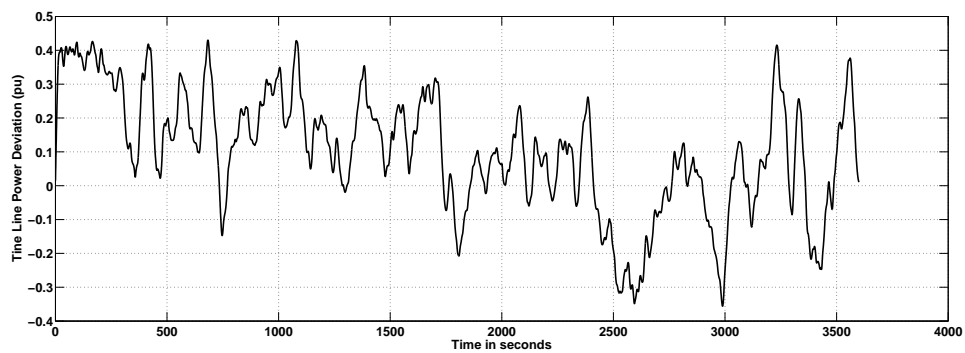


Figure 4.11: Tie Line Power Deviation in Per Unit (generated using the proposed methodology).

Figure 4.12 compares the tie line power deviations in one graph.

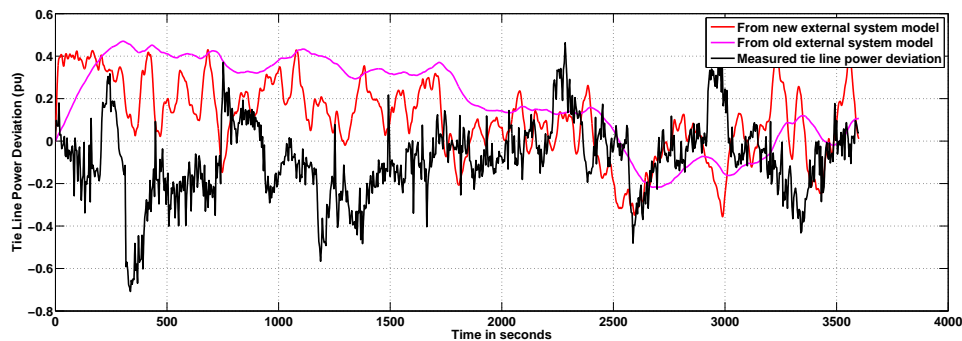


Figure 4.12: Comparison of Tie Line Powers (all quantities are in per unit).

It is evident from Figure 4.10 and Figure 4.11 that the output from the new model is matching closely with the recorded data and thus providing more accurate results than the existing model. The transfer function modeled with the proposed approach, is more sensitive to input changes.

The existing external system and the external system modeled with the proposed methodology is compared with each other in another way. In this comparison the results obtained from the dynamic simulation model of Manitoba Hydro developed in PSS/E is compared with the results that is obtained from the load-frequency control simulation model of Manitoba Hydro developed in PSCAD/EMTDC.

With the change in system load, the tie line power and system frequency may change in a particular manner. For example, when there is a frequency drop in a control area, there is a drop in the tie line power observed from that area too. In the PSS/E dynamic simulation model, few step load changes were provided. Three step load changes as shown in Figure 4.13 were provided to a load at the Manitoba side: one increase, one decrease, and another increase.

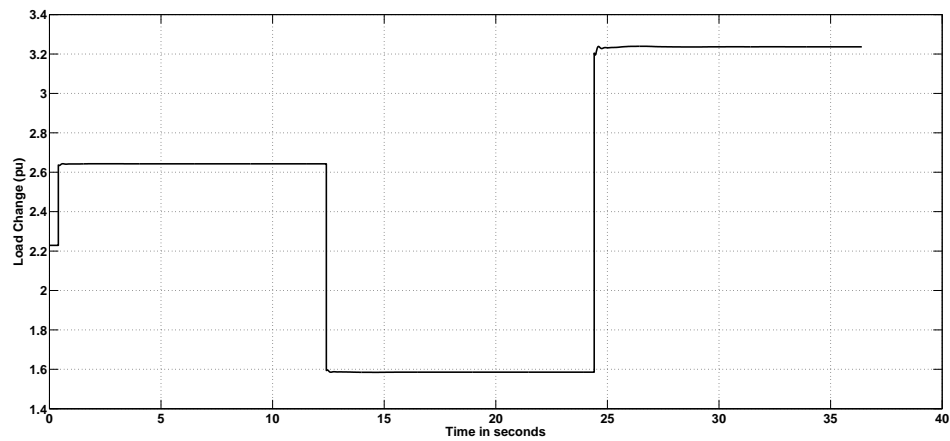


Figure 4.13: Three Step Load Changes.

In response to the load change, the frequency at the border buses which are connected to the two states of USA and the tie line power are observed. Change in load in one control area results in change in system frequency and tie line power. This load change effect on frequency and tie line power are shown in Figures 4.14 and 4.15:

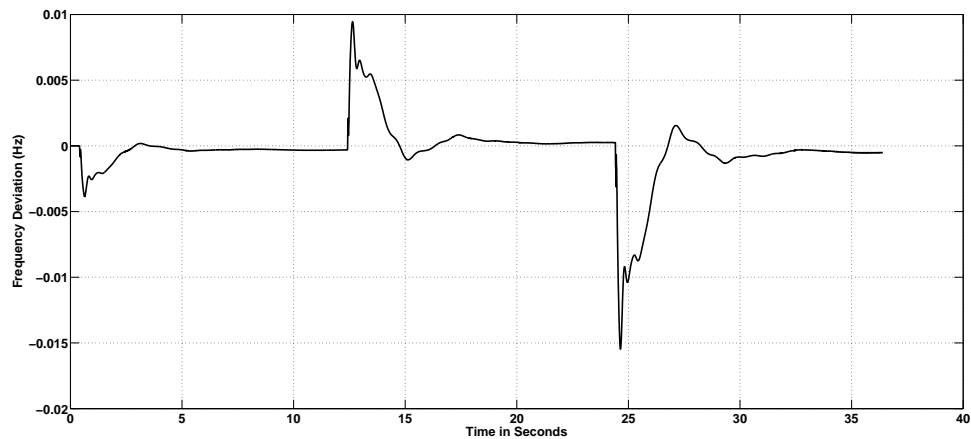


Figure 4.14: Frequency Deviation Following Three Step Load Changes.

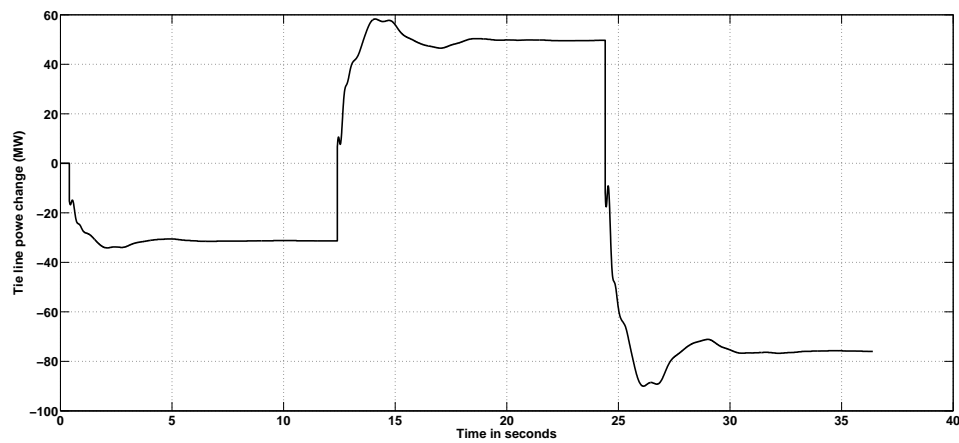


Figure 4.15: Tie Line Power Deviation Following Three Step Load Changes.

A similar study is done in the two area simulation model in PSCAD as described in Section 4.4.2. This model has the external system modeled using the proposed approach in this research. The output from this model is compared with the output from the dynamic simulation model in PSS/E when same input is provided to both.

Eight step load changes as shown in Figure 4.16 were applied to the Manitoba side load.

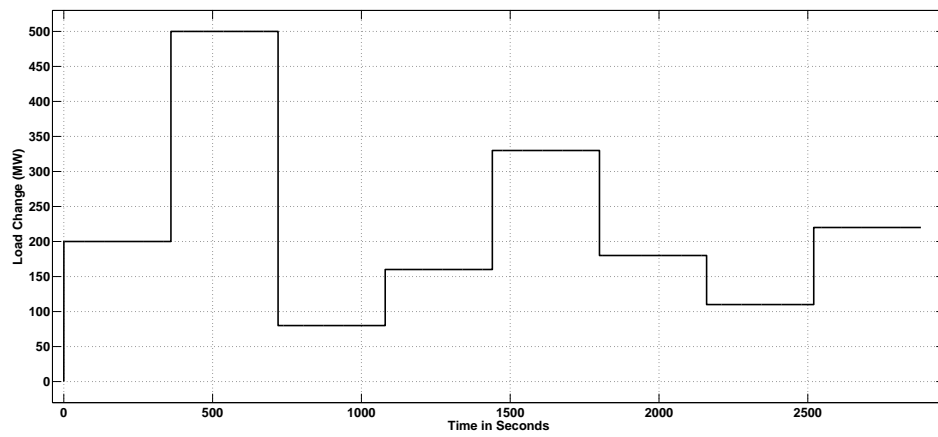


Figure 4.16: Eight Step Load Changes.

In response to the load change the frequency and tie line power deviation is observed and plotted as shown in Figure 4.17.

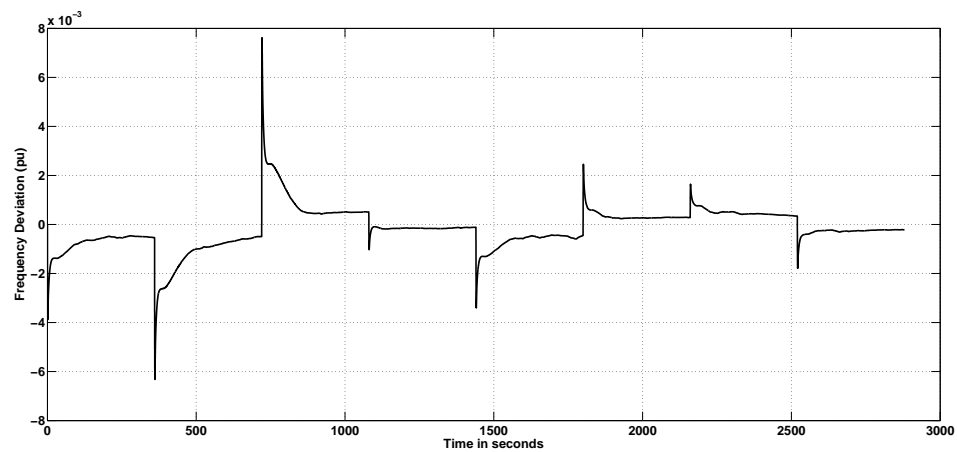


Figure 4.17: Frequency Deviation Following Eight Step Load Changes.

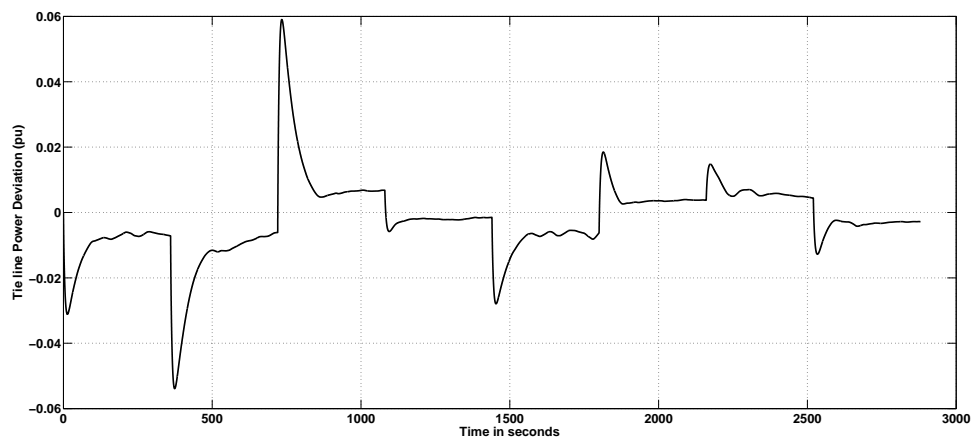


Figure 4.18: Tie Line Power Deviation Following Eight Step Load Changes.

It is observed that in response to the load change the frequency and tie line power changes in the similar direction. In case of an increase in load, the frequency and tie line power decreases. On the other hand if the load is decreased, then the frequency and tie line power increases. These are similar to what is observed from the PSS/E dynamic simulation results. This again shows that the external system model obtained using the new approach produces more accurate results than the existing external system model.

Therefore, if there is a set of measured frequency data, and it is applied to the identified transfer function model, the output tie line power deviation will follow the similar pattern as the input frequency.

Lastly, a frequency deviation as shown in Figure 4.8 is provided to the identified transfer function model as an input to the external system. Figure 4.19 shows the output from the transfer function model.

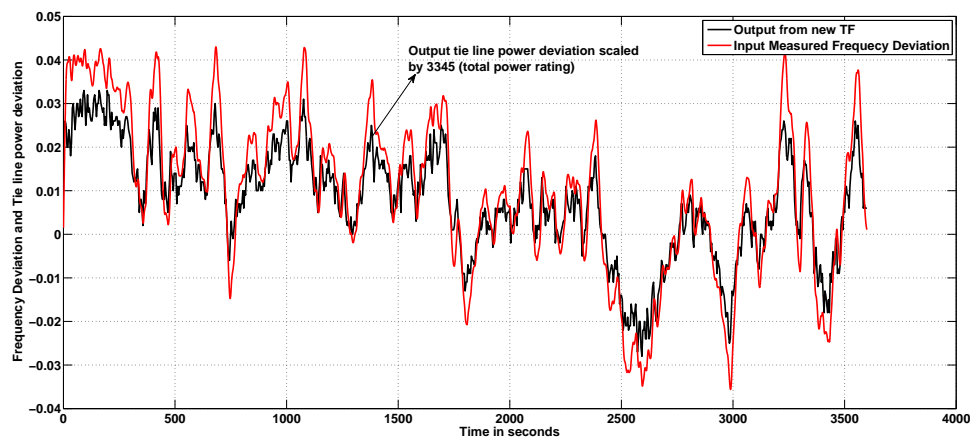


Figure 4.19: Input and Output From The Transfer Function Model is Plotted Together in the Case of New External System Model

The output (which is tie line power deviation) from the model developed using proposed method is scaled to put in the same graph in Figure 4.19 with the frequency deviation data. The purpose is to compare the pattern of these two quantities from the simulation model.

The model produces a tie line power deviation, which follows a pattern similar to the frequency deviation. This is similar to the frequency and tie line power responses showed earlier from the PSS/E dynamic simulation model. On the other hand, the output from the existing external system model for the same input is not demonstrating very accurate results as shown in Figure 4.10. Thus it is certain that the external system developed using the proposed method produces more accurate results.

It can be concluded that the proposed approach of modeling an external system can be used in the Manitoba Hydro time domain simulation model in PSCAD by replacing the existing external system model. This method can be applied in any other intercon-

nected power system.

4.5 Modeling Transfer Functions to Obtain Δf and ΔP for a Practical Power System for the Estimation Purpose of CPS1

4.5.1 Proposed Methodology

In some situations, a load frequency time domain simulation model may not be available. A new method is proposed in this research to overcome the difficulties with that situation for the estimation of CPS1. Electric power utilities have dynamic simulation models of their power system for planning and operational studies. These simulation models are usually modeled with extensive details. A detailed interconnected power system simulation model takes a long period of time to complete a full run even for few seconds. It is not practical and may produce inaccurate results to gather time domain simulation data from a simulation as mentioned above. This research proposes a method to construct two set of transfer functions using System Identification technique to overcome this difficulty.

The two main parameters necessary for the estimation of CPS1 are the frequency deviation Δf and tie line power deviation ΔP . In a power system simulation model a disturbance is provided through a step change in load. Due to the change in load the frequency and tie line power changes. Δf is collected on the border buses between the area under consideration and the one external to it. Similarly ΔP is collected between the tie lines from the area under consideration side to the one external to it. Using System Iden-

tification technique, one transfer function can be constructed using step load changes as input and Δf as output. This transfer function will be able to produce Δf data for the associated power system when a series of step load change is provided. Another transfer function can be modeled using step load change as input and ΔP as output. This transfer function will be able to produce tie line power deviation data when a series of step load change is provided as input. These two transfer functions can produce necessary time domain simulation data for estimation of CPS1 when a set of step load change is provided as input.

An example to demonstrate this proposed methodology is presented in the next section on a practical power system scenario.

4.5.2 Application of the Proposed Methodology

A simulation model is used in this research to validate the results from the proposed methodology. The PSS/E model used for this study is 2011 MRO stability package summer peak cases obtained from Manitoba Hydro. This model is used to obtain necessary data from simulation to apply the *System Identification* technique to estimate transfer function models.

Using the proposed methodology the modeled transfer functions would be able to reproduce the system frequency deviation Δf and tie line power deviation ΔP data when load changes are provided. Using Δf and ΔP data, then CPS1 can be calculated.

The reasons for using the proposed approach are as follows,

1. CPS1 requires clock one minute average values. For this reason long window of

data is necessary.

2. Gathering clock one minute average data for long period of time from a detailed power system simulation model is a time consuming process.
3. Data obtained from a small window of data from a detailed simulation model can contain enough information, which can be used in the System Identification process to model transfer functions to reproduce data for any period of time.

As discussed in Chapter 3, two main components of CPS1 are Δf and ΔP . The relationship between the load change and the frequency deviation and also load change with tie line power deviation is used to model two transfer functions. These two transfer function models can be used to generate frequency deviation and tie line power deviation data for a known/ predicted load distribution provided as an input to those systems. The transfer function models are designed in such a way that they can give realistic results. The reference input and corresponding output is taken from the Manitoba Hydro simulation case as mentioned earlier. The modeled transfer functions are expected to use a load distribution as input. The transfer function models are designed to re-produce estimated data for any duration of time. It is independent of the duration of the actual data set that is used to identify the models. One of the transfer function model will give frequency deviation as output and another transfer function model will use the same input but will produce the tie line power deviation as output. The goal is to estimate and forecast the CPS1 using the data obtained from the transfer function models for future in order to provide useful information in power system planning and operation.

4.5.3 Modeling the Transfer Functions

In order to model the transfer functions, at first necessary data has been collected. Three step load changes as shown in Figure 4.13 were used in these studies. For this load change, the Δf and ΔP responses are obtained. Δf is recorded at the border buses that are located in Manitoba system. ΔP is recorded from the tie lines that connects Manitoba and the US systems. Δf and ΔP from the simulation are same as shown in Figures 4.14 and 4.15, respectively.

It can be seen from the figures that both the frequency and the tie line power is settling down to its steady state after a step change in load within few seconds of time frame. Afterwards, they only change if there is a further change to the system. The data from these graphs are used to model transfer functions which can produce similar frequency deviation and tie line power deviation data followed by step load changes provided to those transfer functions. System Identification technique is used to model the transfer functions.

Two separate transfer functions are estimated using *System Identification* technique. First one with the time domain data of load change as shown in Figure 4.13 as an input data and output as the time domain data of frequency deviation shown in Figure 4.14. This transfer function model is able to reproduce the necessary frequency deviation data when step-load-changes are applied as input. Similarly, the second transfer function can be modeled with time domain data of load change as input and output as the time domain data of tie line power deviation shown in Figure 4.15. This model is able to reproduce tie line power deviation as output data when step-load-changes are provided as input. In both cases, actual value of load change in MW, frequency deviation in Hz, and tie line power deviation in MW is used.

The MATLAB System Identification Toolbox [37] has been used to carry out this operation of estimating the transfer functions. The System Identification toolbox uses least squares method to identify transfer functions with SISO systems. The following are the estimated transfer functions for the two purposes using the proposed method :

$$\frac{-0.0006797s^3 - 0.00266s^2 - 0.01003s - 0.0007889}{s^4 + 7.723s^3 + 64.02s^2 + 95.25s + 135.2} \quad (4.3)$$

$$\frac{-0.3787s^2 - 0.9746s - 1.576}{s^2 + 1.474s + 2.086} \quad (4.4)$$

The transfer function in Equation 4.3 (which can produce frequency deviation data (Δf) for load change) has a fit to estimation data of 86.68% and the transfer function in Equation 4.4, which can produce tie line power deviation data (ΔP) has a fit to estimation data of 97.12%. One of the reason for the frequency deviation related transfer function to have less fit to estimation percentage is the variation of frequency is a very small amount which makes it difficult to model in a lower order transfer function. Figures 4.20 and 4.21 show the comparison between the estimated and the original data curves. The green one is the output from the estimated transfer function and the black one is the actual curve.

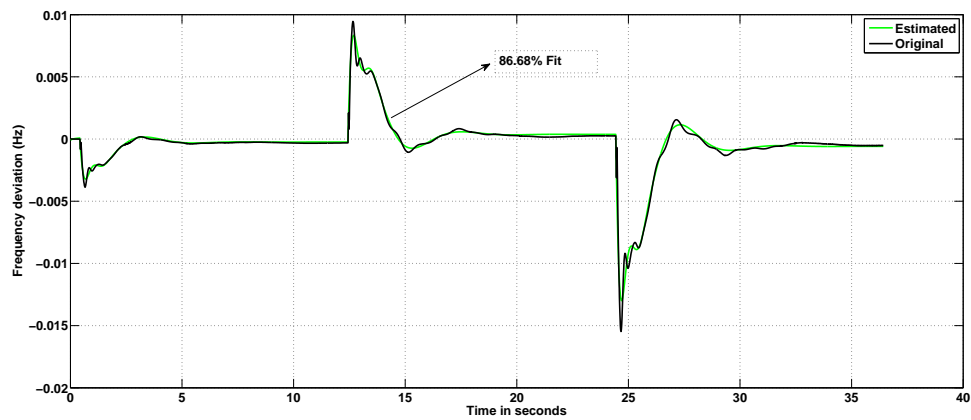


Figure 4.20: Estimated and Original Frequency Deviation Data Curve Comparison.

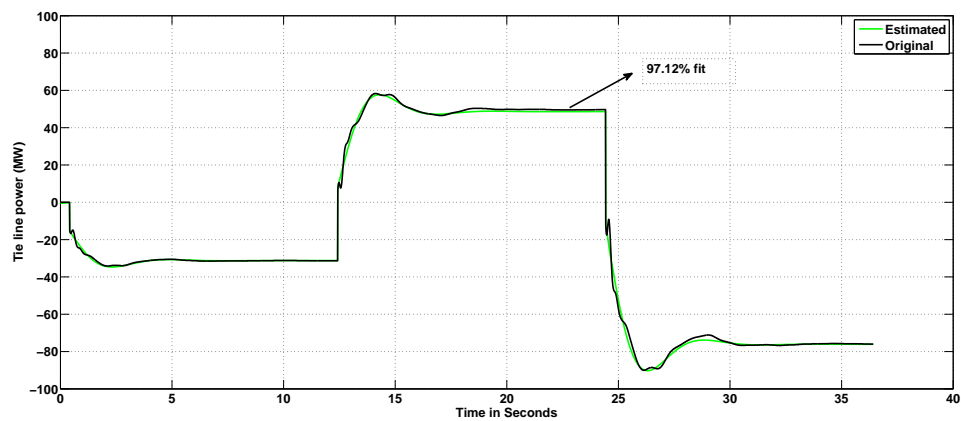


Figure 4.21: Estimated and Original Tie Line Power Deviation Data Curve Comparison.

The above figures show that in both cases, the transfer function models are able to produce the data close to the original data. For both of the transfer functions, the accuracy of estimation is more than 85%.

4.5.3.1 Significance of the Transfer Function Models

These two transfer functions identified using *System Identification* technique are able to produce the Δf and ΔP data when step-load-change is provided as input to them. Transfer function models can provide the data when load change happens at the Manitoba side. The usefulness of these transfer functions are not limited to simple load changes. The load change distribution which is provided as the input to the modeled transfer functions can be modified to capture different effects. For example, to capture the wind generation effect from the USA interconnection to Manitoba CPS1, it can be added as a negative load to the load change distribution in Manitoba side. This distribution can then be used as an input to the modeled transfer functions to gather data and estimate CPS1. The resulted CPS1 will reflect the effect of wind penetration from the US interconnection.

The proposed method of modeling transfer functions using System Identification technique to obtain necessary time domain simulation data to estimate frequency control performance index can be used in any power system provided that a detailed up-to-date dynamic simulation model is available

4.6 Summary and Conclusions

In this Chapter, details about various aspects of System Identification technique are discussed. A brief theory behind System Identification is presented. The application of the System Identification is also explained. Two methods to estimate transfer function models using System Identification technique that can be used to estimate CPS1 are presented.

The first method can be applied when a load-frequency time domain simulation of an interconnected power system for estimation of CPS1 is available. The proposed approach uses a dynamic simulation model of a power system to obtain necessary up-to-date data to apply System Identification technique. The new method models an accurate approximate equivalent power system external to a system under consideration. The second method uses System Identification to model two transfer functions to produce necessary data for the estimation of CPS1. Using this method it is possible to eliminate the issues related with running a detailed power system simulation for long period of time. The proposed methods were validated using simulation results. A North American Electric Power utility's simulation model is used as an example to show the validity of the proposed methods.

The next chapter presents the details of the estimation process for CPS1.

Chapter 5

Estimation of Control Performance Standard 1 (CPS1)

5.1 Introduction

In Chapter 4, System Identification and its application is presented. Two methods are proposed for the purpose of estimation of CPS1. This chapter explains the estimation of CPS1 using the PDF method proposed in [10] which is applied for a practical power system. The results obtained from the PDF method are validated against those obtained from time domain simulation for two cases. The applicability of PDF method proposed in [10] is tested for a practical power system which is one of the significant contributions of this thesis. Study results presented in this thesis show that the value of CPS1 index depends mainly on the load change amount, and its dependency on the value of the actual load is not significant.

It is also shown that the components of the CPS1 are sensitive to the change in load and thus a change in load has a direct effect on the value of CPS1. The main objectives of this chapter are as follows:

- Estimation of CPS1 for a large practical interconnected power system without running a detailed power system simulation.
- To calculate the CPS1 directly from the probability distribution of the load change without running a time domain simulation using the method from [10], [11] for a practical power system.

This chapter examines the approximate relationship between clock-one-minute values of Compliance Factor (CF) and the magnitude of a step load change in a practical power system [10]. This relationship is independent of time under certain assumptions. The relationship is useful to estimate the CPS1 value fairly accurately compared to the time domain simulation results. This way the CPS1 can be estimated in a much more faster and simpler process.

5.2 Relationship Between a Single Step Load Change With CF and It's Components

In Chapter 3, it is shown that CPS1 has a linear relationship with both clock one minute values of CF and clock one minute average value of CF[10]. In this thesis the clock-one-minute-average value of CF is designated as CF_{1M} . In this section the relationship between CF_{1M} and a single step load change is initially demonstrated using the load frequency simulation model described in Section 4.4.2 of Chapter 4 . Chapter 3 shows that the CF_{1M} is a function of clock one minute average values of frequency deviation Δf_{1M} and clock one minute average values of tie line power deviation ΔP_{1M} . Initially, the relationship between Δf_{1M} , ΔP_{1M} , and a single step load change is established by observing frequency deviation (Δf) and tie line power deviation (ΔP) profiles for various

magnitudes of step-load-changes. This association is then used to set up the relationship between Δf_{1M} , ΔP_{1M} , CF_{1M} and a single step load change.

5.2.1 Relationship Between Δf_{1M} , ΔP_{1m} , and the Magnitude of a Single-Step-Load-Change

Load frequency simulation model that is introduced in Section 4.4.2 of Chapter 4 is modeled as a linear control system. Therefore, there is a linear relationship between any amount of a single step load change with Δf and ΔP . This leads to the fact that if the time variation of Δf for a specific amount of load change is known, then the time variation of Δf for other amount of load changes can also be estimated, unless the limits of the control system (i.e. maximum/minimum outputs of generators, ramp rates, dead-band of the governor etc.) are reached. This relationship can be demonstrated by applying three different step load changes of 100 MW, 500 MW, and 1000 MW that were examined using the time domain simulation model. Load changes were applied separately one at a time. The data for Δf and ΔP with respect to time were obtained from this simulation model for a period of 200 seconds.

Δf and ΔP at any instant is denoted by Δf^i and ΔP^i , respectively. Where 'i' denotes the specific time instant. The following relationship is observed and proved to be true at any given instant of time for the total simulation period.

$$\frac{(\Delta f^i)_{1000MW_change}}{(\Delta f^i)_{100MW_change}} = 10 \text{ and } \frac{(\Delta f^i)_{500MW_change}}{(\Delta f^i)_{100MW_change}} = 5$$

$$\frac{(\Delta P^i)_{1000MW_change}}{(\Delta P^i)_{100MW_change}} = 10 \text{ and } \frac{(\Delta P^i)_{500MW_change}}{(\Delta f^i)_{100MW_change}} = 5$$

The Δf and ΔP variations for different step load changes is further illustrated in graphs to show the linear relationship in Figures 5.1 and 5.2

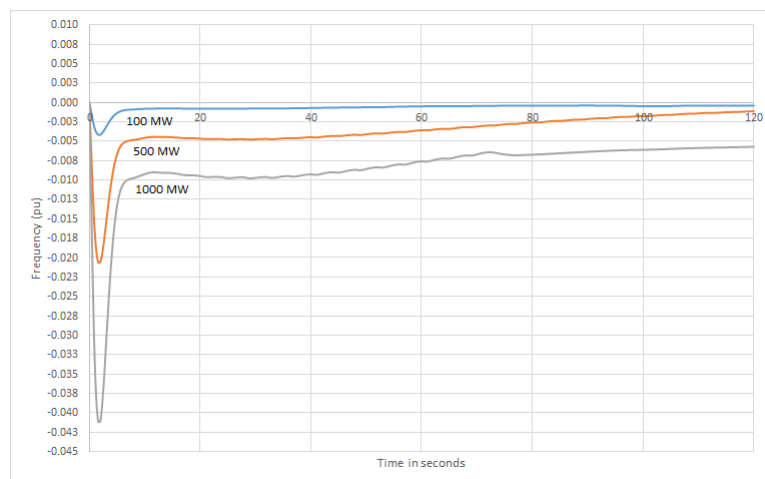


Figure 5.1: ΔF^i For Load Increase in Manitoba Area.

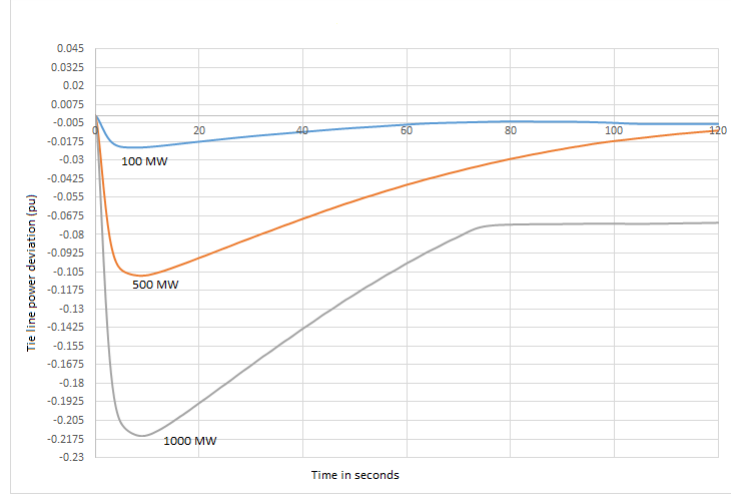


Figure 5.2: ΔP^i For Load Increase in Manitoba Area.

It can be seen from Figures 5.1 and 5.2 that time variation of Δf^i and ΔP^i for a 500 MW step load change can be obtained by scaling respective profiles of 100 MW step load change by 5 or for 1000 MW load change profile by 10. Similarly, for any other step load change appropriate scaling can be used to obtain the target values of Δf and ΔP .

It is evident that the clock-one-minute average values of Δf and ΔP will also maintain the same linear relationship. That means for two different step load changes in Manitoba area Δf_{1M} and ΔP_{1M} values are linearly proportional to the corresponding magnitudes of the step load changes. This linear property is illustrated in Figures 5.3 and 5.4

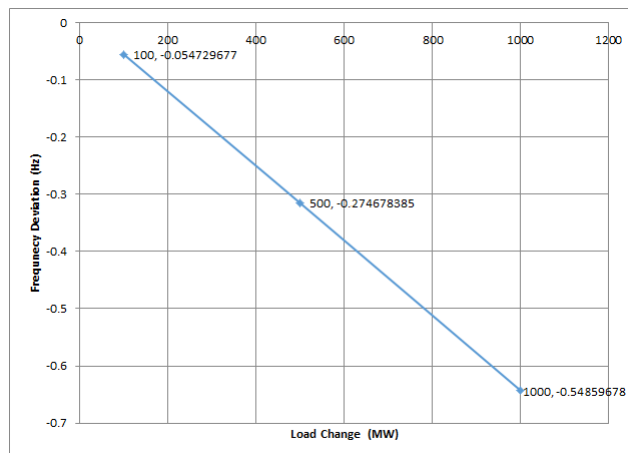


Figure 5.3: Clock-One-Minute-Average Value of Δf for the First Minute.

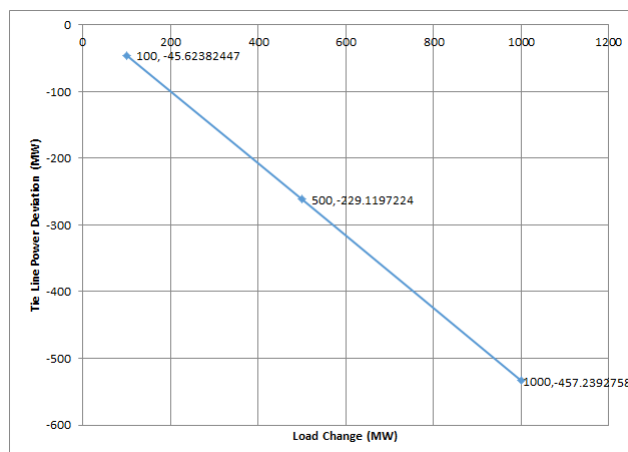


Figure 5.4: Clock-One-Minute-Average Value of ΔP for the First Minute.

5.2.2 Relationship of Single-Step-Load-Change With CF_{1M}

The summary of the relationship between CF_{1M} and its components from Equation 3.7 can be stated as follows:

- CF_{1M} is linearly proportional to the term, $(\Delta P_{1M} * \Delta f_{1M}) + (\Delta f_{1M})^2$
- Δf_{1M} and ΔP_{1M} are linearly proportional to a single-step load change.

It can be, therefore, concluded that the clock-one-minute average value of the compliance factor for a single-step load change is a *quadratic* function of the magnitude of the step load change.

Figure 5.5 illustrates CF_{1M} for the first minute for different load changes. The load change magnitudes are 100 MW, 500 MW, and 1000 MW. The data points are connected with a single line and the points are shown as solid dots.

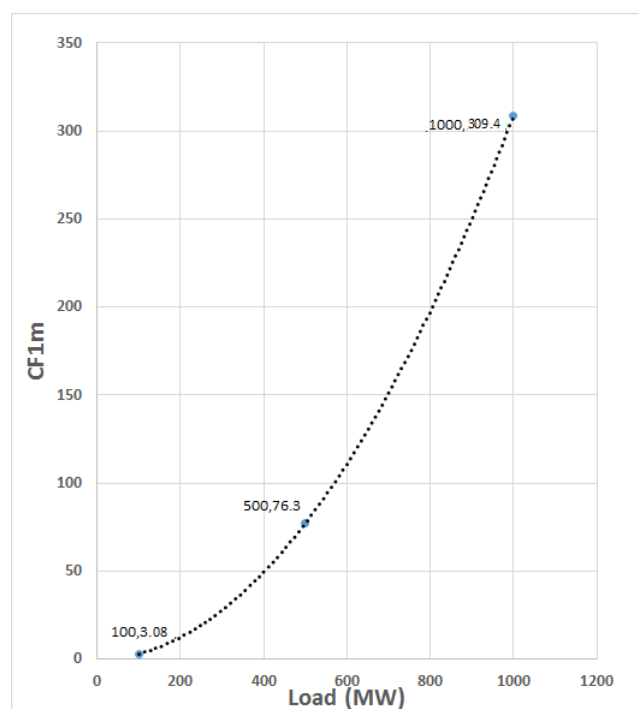


Figure 5.5: CF_{1M} for the First Minute for Different Load Changes.

It can be seen from Figure 5.5 that the relationship of CF_{1M} and step load change can be represented as:

$$CF_{1M} = \Lambda(\Delta P_L)^2 \quad (5.1)$$

Where, Λ is a constant and ΔP_L is the magnitude of the step load change. The line connecting the dots in Figure 5.5 represent the quadratic function.

5.3 Significant Period of CF_{1M}

Magnitudes of the CF_{1M} after a load change gradually decrease and settles to a value close to zero. This is because the transients caused by the load change slowly die down. Therefore, CF_{1M} values after a few minutes are not as significant and can be ignored during the calculation process of CPS1 without causing significant error.

To demonstrate the above mentioned fact, different step load changes are applied to the Manitoba control area of the load frequency model that is introduced in Chapter 4 Section 4.4.2. Table 5.1 shows the CF_{1M} values for Manitoba control area. It can be seen from Table 5.1 that the 2nd minute CF_{1M} is negligible as compared to the 1st minute of CF_{1M} .

Table 5.1: CF_{1M} values

Step Load Change (MW)	CF_{1M} 1st minute (pu)	CF_{1M} 2nd minute (pu)
1000	36.667	0.307
500	9.17	0.0779
100	0.367	3.062×10^{-3}

5.4 Estimation of CF and It's Components for a Multi-Step-Load-Change

Following this section, the rest of the chapter demonstrates the calculation of the CF_{1M} and CPS1 for multi-step load change based on the relationship established between Δf , ΔP , CF_{1M} , and single-step-load-change in Sections 5.2 and 5.3. The PDF method proposed in [10] [11] to calculate CF_{1M} and CPS1 was validated only for a simple two-area simulation model. In this chapter the PDF method is applied to the interconnected power system simulation model that is introduced in Section 4.4.2 of Chapter 4. It shows that the PDF method can successfully be used to estimate CPS1 for a large and more complicated power system.

The PDF method is also applied in a situation where a time domain simulation model is not available. In this case, the transfer functions that is modeled using the proposed methodology as described in Section 4.5 is used to obtain the necessary parameters for estimation of CPS1.

5.4.1 Estimation of CF_{1M} When a Time Domain Simulation Model is Available

A measured set of load change data is obtained from Manitoba Hydro and is used in this study. This data was recorded for an hour in May 2007. It is sampled with a constant time interval of 3 minutes, therefore 20 step load changes were taken to develop a load change distribution (assuming that the load does not vary between any two sampling points.) The multi-step load change is portrayed in Figure 5.6.

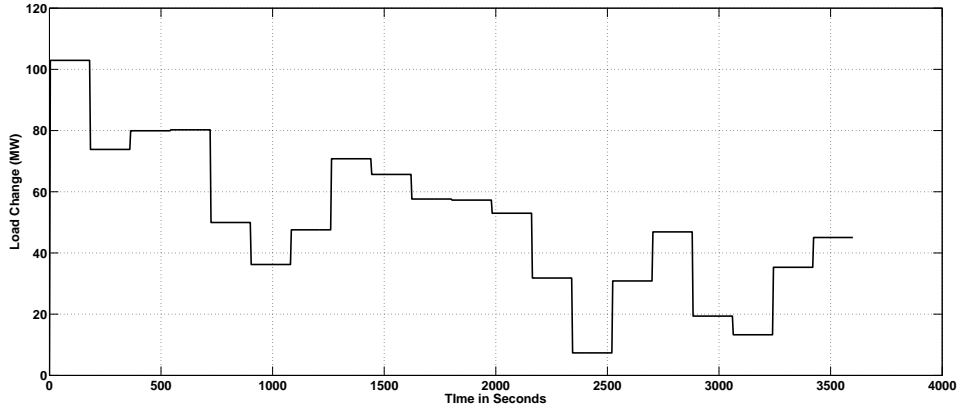


Figure 5.6: Twenty-Step-Load-Change.

The load change distribution is applied to the Manitoba control area of the time domain simulation model as described in Section 4.5. In response to the load change, Δf and ΔP are obtained from the simulation. With the obtained data the CF_{1M} is calculated using Equation 3.3. Calculated CF_{1M} values are negligible after 2-3 minutes as compared to the CF_{1M} values of the first minute. Thus, only the first three minutes CF_{1M} values were used. For the same reason, the time span between consecutive load changes were taken as 3 minutes. So for each load change, the CF_{1M} values for first three minutes were summed, then CF_{1M} values for all the load changes were summed and then averaged over the total time span in minutes, which is 60 minutes in this case.

This can be represented by the following equation:

$$CF_{avg} = \frac{\sum CF \text{ of each load change}}{\text{Total time span of the load changes in minutes}} \quad (5.2)$$

After calculation of the CF_{1M} , using Equation 3.2 the CPS1 can be estimated. This is the CPS1 result obtained from the time domain simulation. This result is compared with the CPS1 estimated using PDF method. The estimation process of CPS1 using

PDF method is described as below.

It is noted that in Sections 5.2 and 5.3, CF_{1M} values for single-step-load-changes are proportional to the square of the magnitudes of the corresponding load changes. The proportionality constant that relates the CF_{1M} and a single step load change could be found if CF_{1M} values for any single-step-load load change is known. CF_{1M} contribution in response to each load change could be calculated using the quadratic relationship between CF_{1M} and single-step-load-change. This is demonstrated below where the average CF_{1M} values are estimated using Equation 5.1.

In order to estimate the average CF_{1M} values for the multi-step-load-change given in Figure 5.6, CF_{1M} values for a 80.24 MW step-load-change is used. This CF_{1M} value can be scaled and CF_{1M} for any other load change can be obtained using the quadratic relationship between CF_{1M} and load change.

$$CF_{avg} = \frac{1}{m * N} * \sum \left(\left(\frac{\Delta P_L}{K} \right)^2 * CF_x * n_A \right) \quad (5.3)$$

Where,

m is the time span between two consecutive step-load-change

N is the total number of load changes in that area

ΔP_L is the magnitude of the step load change

K is the magnitude of step-load-change for which the CF_x is known

CF_x is the CF_{1M} which is known for a single step load change of magnitude x

n_A is the number of load changes in a area with magnitude ΔP_L .

The comparison of CPS1 value including the percentage of error between PDF method and Time domain (TD) simulation results is shown in Table 5.2. The error in CPS1 is

less than 0.0002% for the 60 minutes period considered in the above example.

Table 5.2: Comparison of CPS1 Values When the First Method is Applied

	PDF method	TD simulation	% Error
<i>CPS1</i>	199.98	199.949	0.00015

Therefore, it is proven that the PDF method presented in references [10] and [11] can be applied in a larger and more complicated power system without significant error. CPS1 can be estimated for a multi-step-load-change, when the area-load-change data is available with time span between consecutive load changes, and CF_{1M} value for any single-step-load change is provided.

5.4.2 Estimation and Validation of CF_{1M} and CPS1 Using Data from Transfer Function Models

Using the proposed method in Section 4.5, two transfer functions were modeled in Chapter 4 to produce Δf and ΔP data. Transient stability simulation model for Manitoba Hydro and its interconnected system is used to gather data for the transfer function identification process. The used model represents the 2012 summer peak operating condition. The transfer function models are able to produce data for any duration of time depending on the provided input. Using MATLAB Random Number Generation Tool, a uniform distribution of 20 step load changes were generated as shown in Figure 5.7 and provided as an input to the transfer functions. In this case each step load change is provided for 2 minutes duration to the transfer function models. The reason is that the transients die down by that time and the calculated value of compliance factor is very negligible afterwards.

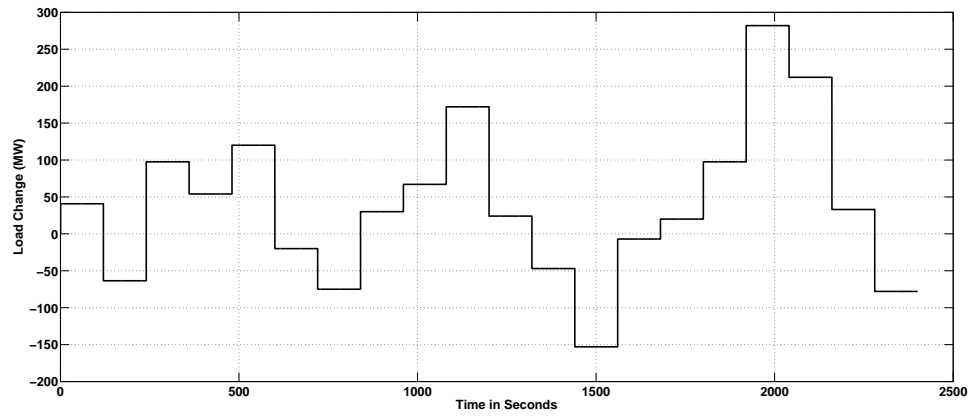


Figure 5.7: Random Load Change Provided to the System.

Due to this load change, the system frequency and the tie line power interchange varies. When this load change is provided to the transfer function models as described by Equations 4.3 and 4.4 the output frequency deviation and tie line power deviation are shown in Figures 5.8 and 5.9

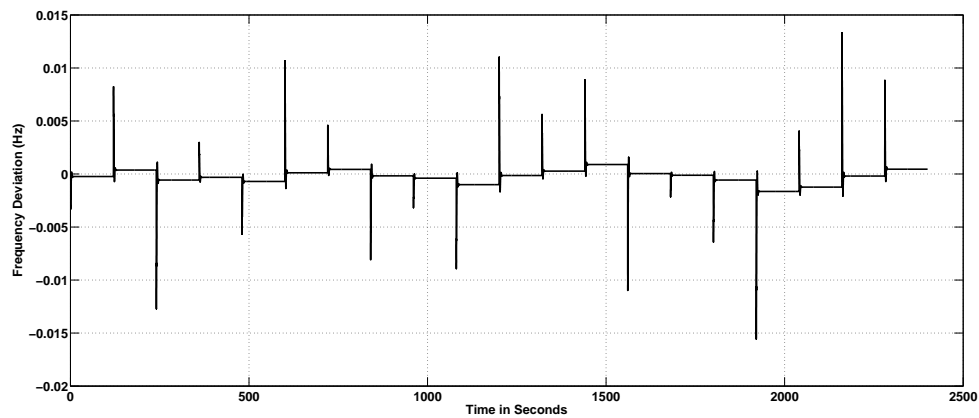


Figure 5.8: Frequency Deviation for 20 Step Load Changes.

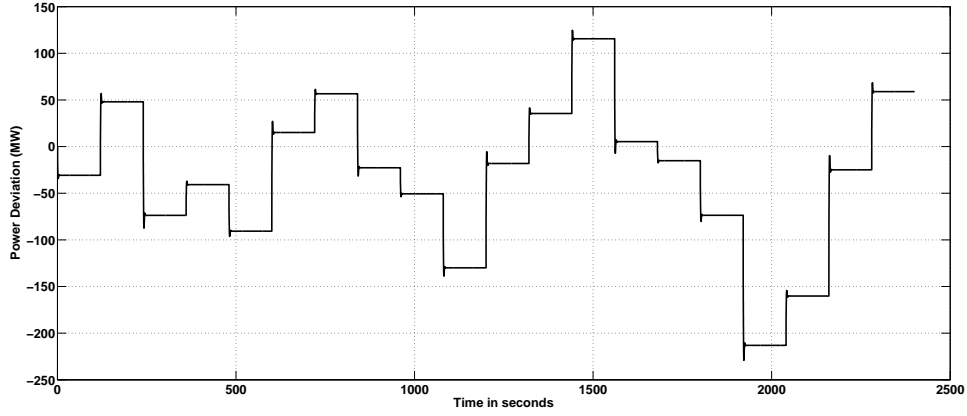


Figure 5.9: Tie Line Power Deviation for 20 Step Load Changes.

Using data from above graphs obtained from time domain simulation and Equation 3.3, compliance factors for each load change can be calculated. Then the total compliance factor can be divided with the total time span in minutes (which is 40 minutes in this case) to get the average compliance factor for 20 step load changes. Using Equation 3.2, CPS1 can be calculated from the CF values. The CPS1 estimated using the PDF method is validated against those obtained from time domain simulation.

The PDF method requires calculating CF for one of the step load changes from the time domain simulation. In this case, to estimate the CF_{1M} values for the multi-step-load-changes given in Figure 5.7, CF_{1M} values for a 40.74 MW load change is used. Table 5.3 shows the CF_{1M} values that is used for the calculation purpose.

Table 5.3: CF_{1M} Values used for PDF Method

	1st minute	2nd minute	Sum of CF_{1M} for first two minutes
CF_{1M}	0.059	0.049	0.109

CF_{1M} value shown in Table 5.3 can be scaled based on the quadratic relationship be-

tween CF_{1M} and load change to get the sum of CF_{1M} for other single-step-load-changes. This value depends on the system operating point and can also change depending on the load deviation from its nominal value. The CF_{1M} for the multi-step-load-changes as shown in Figure 5.7 is calculated using Equation 5.3. After CF_{1M} is calculated, CPS1 can be estimated using Equation 3.2.

Table 5.4 shows the CF_{1M} values obtained from PDF method and compares with time domain simulation results. The error between these two results are also shown in the table. This error is approximately 5%, which is considered to be within the acceptable range. One of the main reasons for this error is due to finite sample size of load-changes that was used in the estimation.

Table 5.4: Comparison of CF_{1M} Values When the Second Method is Applied

	PDF method	TD simulation	% Error
CF_{1M}	0.396	0.378	4.644

Table 5.5 compares the CPS1 values obtained using the PDF method and time domain simulation. In this case, the error is approximately 1.1% which is considered to be within acceptable range as well.

Table 5.5: Comparison of CPS1 Values When the Second Method is Applied

	PDF method	TD simulation	% Error
$CPS1$	160.445	162.201	-1.083

It can be concluded from above analysis that the average CF_{1M} and CPS1 for a practical electric power utility company can be estimated when a probability distribution of load change is given. Although this conclusion was drawn based on the study results

obtained using data from Manitoba Hydro, similar approach can be applied to any other power utility system for the estimation of frequency control performance indices. The study results show that the estimation process does not produce significant error as compared to the time domain simulation.

5.5 Summary and Conclusions

It is shown in this chapter that PDF method of estimating CPS1 can be used in a practical interconnected power system. The results obtained from the PDF method are compared with those obtained from time domain simulation. The comparison shows that the error is negligible. It can be concluded that the PDF method can be used for a practical power system to estimate CPS1 when a load change distribution is available.

Some remarks and conclusion of this thesis along with future works are mentioned in the next chapter.

Chapter 6

Summary and Conclusions

6.1 Summary

Chapter 1 provides some background information including the development and the importance of power system interconnected operation, power system load-frequency control and evaluation of power system frequency performance using the CPS1 and CPS2 indices. This chapter also discusses the motivation of the work and lays out the objectives of the research.

Chapter 2 provides an overview of main control functions of a typical power system. This chapter discusses load change response to changes in generators providing active power and to changes in frequency due to load changes. The three levels of frequency controls and their importance are presented. The contents of this chapter provides useful information for the analysis of NERC CPS indices.

Chapter 3 discusses the CPS1 index, its components and the relationship with each other in more detail. Relationship between ΔP , Δf with CF is presented in this chapter.

This relationship enables to calculate CF with ΔP and Δf data. This chapter also shows CPS1 value for different ranges of ΔP and Δf which is useful to relate an average power system behavior with CF.

In Chapter 4, various aspects of System Identification technique are discussed. Brief theory of System Identification and the application of the technique in this research is presented. Two methods to estimate transfer function models using System Identification technique that can be used to estimate CPS1 are proposed and validated with study results. The first method proposes to develop a more accurate approximate equivalent transfer function model of a power system external to a system under consideration. The second method is proposed to develop two transfer functions to produce necessary data for the estimation of CPS1. The proposed methods were validated using simulation results. A practical power system dynamic simulation model is used as an example to show the validity of the proposed methods.

Chapter 5 discusses estimation of CPS1 for a future time using both the PDF method and the traditional time domain simulation. In this chapter the proposed methods in Chapter 4 are used for the estimation process of CPS1. It is shown that using the PDF method, CPS1 for a large practical power system can be estimated accurately when a probability distribution of load change is available. The results obtained from the PDF method is compared with those obtained from traditional time domain simulation. It is shown that the difference between the results obtained using these two estimation process is negligible.

6.2 Contributions

This thesis proposes two methods to estimate transfer function models using System Identification technique that can be used to estimate CPS1. The first method is applicable when a load-frequency time domain simulation of an interconnected power system for estimation of CPS1 is available. This approach uses a dynamic simulation model of a power system to obtain necessary up-to-date data to apply system identification technique. The new method models an accurate approximate equivalent power system external to a system under consideration. This enables the assessment of frequency control performance for a control area in an interconnected power system more accurately. It also helps to have an enhanced load-frequency model which can be used for various types of studies. For example studies related with integration of wind generation to the current system, studies related with optimization of regulating reserve management etc.

The second method is applicable when a time domain simulation model for the estimation of CPS1 is not available. This method uses System Identification to model two transfer functions to produce necessary data for the estimation of CPS1. The necessary up-to-date data for System Identification is obtained from available dynamic simulation model. Each step of the proposed approach is explained using simulation results. For simulation example, an actual power system simulation model is used. Using this method it is possible to eliminate the issues related with running a detailed power system simulation for long period of time. This is one of the major contributions of this research.

CPS1 estimation process and calculated results is also presented in this thesis. The results obtained using the PDF method presented in references [10], [11] are compared with those calculated using time domain simulation results. This research shows that frequency control performance index of a practical interconnected power system can be

estimated using probability distribution of load change without running a time domain simulation. It is evident that the method is reliable and CPS1 could be approximated without significant error.

6.3 Future Work

The research approach has been applied to an actual power system and the results are validated. The power system model in the PSS/E simulation program that is used, does not have the Automatic Generation Control (AGC) modeled in it. A user written AGC model can be developed in the future to enhance the current model and this approach of calculating the control performance index can be applied to carry out further studies. The impact of AGC operation on CPS1 index can be examined.

The research can be expanded to find a way to optimize the regulating reserve of a control area of an interconnected power system. Finding out possible solutions for assessing CPS2 index can be done in the future.

Abbreviations

- **CPS** Control Performance Standard
- **NERC** North American Electric Reliability Corporation
- **CPC** Control Performance Criteria
- **ACE** Area Control Error
- **AGC** Automatic Generation Control
- **CF** Compliance Factor
- **HVDC** High Voltage Direct Current
- **SVC** Static VAR Compensator
- **STATCOM** Static Synchronous Compensator
- **PSSE** Power System Simulator for Engineering

Appendix A

System Identification

A.1 Types of System Identification Technique

Currently there are various type of system identification technique available. There are traditional methods of linear system identification, and then modern methods of non linear system identification [39].

Among the traditional methods, the most commonly used ones are the following:

1. Least Squares Method.
2. Gradient Correction Method.
3. Maximum Likelihood Method.

The advantages of the above mentioned identification methods are as following,

- Generalized error criterion function is taken as the criterion function and impact of system noise needs to be taken into account in the process of identification.
- Pseudo random signal can be used as input signal even though Gaussian white noise is the theoretical input signal.

- They are very useful for online identification.

The disadvantages of these traditional methods are,

- Input signal has to be known for the least square method.
- Input signal has to change richly and relatively, in some dynamic systems this condition is hard to satisfy.
- These methods are more accurate in the linear systems than non linear cases.
- A synchronization between structure identification and parameter identification cannot be readily achieved.

Modern methods for nonlinear system identification techniques include,

1. Neural logic identification method.
2. Fuzzy logic identification method.
3. Genetic algorithm based identification method.
4. Swarm intelligence optimization algorithm based identification method.
5. Auxiliary model identification method.
6. Multi innovation identification method.
7. Hierarchical Identification method.

The main advantages of the modern methods of system identification is that these methods can be used to identify both non linear and linear systems. Whereas the traditional methods are mostly applicable for linear system identification. A real power system is complicated and non linear. But in this thesis for the CPS1 estimation purpose the

system of interest is assumed to be of linear characteristics. A linear identification technique is applied to the system. Thus the non linear system identification methods are not going to be discussed further.

To optimally fit the model to the system data the defined error criterion needs to be minimized. There are different ways to define an error. Such as the deviation of the parameter estimates from the true values (parameter error), or the difference between the output of the system and that of the model in response to the same input (output error), or as the discrepancy between the model equation and the measured input and output data (equation error). In many cases the equation error is the most commonly used one.

Two types of mode exist to accomplish the system identification. One is *off line identification*, in which a record of input-output data is initially observed and then the model parameters are estimated based on the entire recorded data. On the other hand, *on-line identification*, the parameter estimates are recursively calculated for every data set so that the new data can be used to correct and update the existing estimates. If the updating process can be made very fast, it becomes possible to obtain parameter estimates of time varying systems with reasonable accuracy. This capability is called *on-line real-time identification*.

In this research the least squares method is chosen to be used for number of reasons. This method is a very familiar method with which scientific workers in many disciplines are familiar with. The least squares method is appealing in that it offers conceptual simplicity and applicability to a wide variety of situations in which other statistical-estimation theories might be difficult to apply, yet it exhibits very strong statistical properties. This method can also be related to other identification techniques making possible a unified

treatment of the system identification problem. In this particular identification problem described in the thesis the input signal is known, and the system characteristic is assumed to be linear. In these situation the best suited method to be used is chosen as *Least Squares Method*.

A.2 Least Squares Theory

The least-squares technique provides a mathematical procedure by which a model can achieve a best fit to experimental data in the sense of minimum-error-squares[35]. Lets assume there is a variable y which is linearly related to n set of variables $x = (x_1, x_2, \dots, x_n)$, that is,

$$y = \theta_1 x_1 + \theta_2 x_2 + \dots + \theta_n x_n \quad (\text{A.1})$$

Where $\theta = (\theta_1, \theta_2, \dots, \theta_n)$ is a constant parameter set. It is assumed that θ_i are unknown and it is needed to estimate their values by observing the variables y and x at different times. This problem can be represented in a block diagram

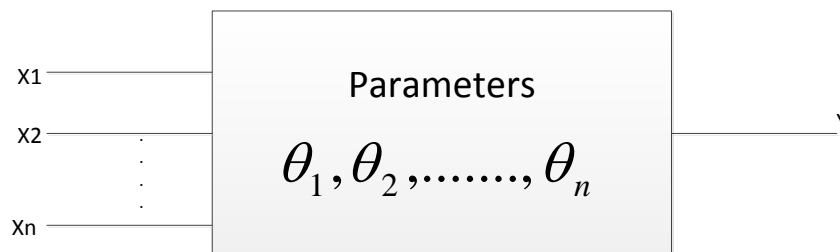


Figure A.1: An n -parameter Linear System.

Assuming that a sequence of m observations on both y and x has been made at

times t_1, t_2, \dots, t_m , and denoting the measured data by $y(i)$ and $(x_1(i), x_2(i), \dots, x_n(i))$, $i = 1, 2, 3, \dots, m$. These data can be related with the following set of m linear equations,

$$y(i) = \theta_1 x_1(i) + \theta_2 x_2(i) + \dots + \theta_n x_n(i) \quad i = 1, 2, \dots, m \quad (\text{A.2})$$

In the statistical literature, equation A.2 is called a regression function, and θ_i are the regression coefficients.

The system equations A.2 can be arranged into a simple matrix form,

$$y = X\theta \quad (\text{A.3})$$

$$y = \begin{bmatrix} y(1) \\ y(2) \\ \cdot \\ \cdot \\ \cdot \\ y(m) \end{bmatrix} \quad X = \begin{bmatrix} x_1(1) & \dots & x_n(1) \\ x_1(2) & & x_n(2) \\ \cdot & & \cdot \\ \cdot & & \cdot \\ \cdot & & \cdot \\ x_1(m) & \dots & x_n(m) \end{bmatrix} \quad \theta = \begin{bmatrix} \theta_1 \\ \theta_2 \\ \cdot \\ \cdot \\ \cdot \\ \theta_n \end{bmatrix} \quad (\text{A.4})$$

For the estimation of the n parameters of θ , it is necessary that $m \geq n$. If $m = n$, then θ can be solved uniquely from equation A.3 by,

$$\hat{\theta} = X^{-1}y \quad (\text{A.5})$$

Where X^{-1} is the inverse of the square matrix X . $\hat{\theta}$ denotes the estimation of θ . However, when $m > n$, it is usually not possible to obtain a set of θ_i exactly satisfying all m equations A.2, as the data could be disturbed with random noise. In this respect the problem can be resolved by determining θ with the help of least-squares error.

Defining an error vector $\epsilon = (\epsilon_1, \epsilon_2, \dots, \epsilon_m)^T$ and assuming

$$\epsilon = y - X\theta \quad (\text{A.6})$$

$\hat{\theta}$ can be chosen such a way so that the criterion J can be defined as follows,

$$J = \sum_{i=1}^m \epsilon_i^2 = \epsilon^T \epsilon \quad (\text{A.7})$$

This J can be minimized, and in order to do that J can be expressed as,

$$J = (y - X\theta)^T(y - X\theta) = y^T y - \theta^T X^T y - y^T X \theta + \theta^T X^T X \theta \quad (\text{A.8})$$

Differentiating J with respect to θ and then equating the result to zero would lead to determine the conditions for the estimations of $\hat{\theta}$ which will minimize J . Thus,

$$\left. \frac{\partial J}{\partial \theta} \right|_{\theta=\hat{\theta}} = -2X^T y + 2X^T X \hat{\theta} \quad (\text{A.9})$$

This yields,

$$X^T X \hat{\theta} = X^T y \quad (\text{A.10})$$

from which the solution for $\hat{\theta}$ can be obtained as,

$$\hat{\theta} = (X^T X)^{-1} X^T y \quad (\text{A.11})$$

This result is called the *least squares estimator* (LSE) of θ . Equation A.10 is referred to as the *normal equation* and ϵ is called as the *residual* in statistical literature.

This above result is derived based on the criterion J that weights all the error ϵ_i in an equal manner. This result is often referred to as *ordinary least squares*. If each error

term needs to be weighted differently a separate variable can be added to the equation A.7. Let W be the desired weighting matrix. Therefore, the weighting criterion becomes,

$$J_W = \epsilon^T W \epsilon = (y - X\theta)^T W (y - X\theta) \quad (\text{A.12})$$

Here W is restricted to being a symmetric positive definite matrix. If minimized J_W with respect to θ yields the *weighted least squares estimator* (WLSE) of $\hat{\theta}_W$,

$$\hat{\theta}_W = (X^T W X)^{-1} X^T W y \quad (\text{A.13})$$

It is observed that when W is chosen as an identity matrix I , $\hat{\theta}_W$ is reduced to only $\hat{\theta}$.

A.3 Statistical Properties of Least Squares Estimators

The least squares method that has been derived above is examined to check its qualities in this section[35]. Equation A.6 is analyzed in which the vector ϵ is included to account for the measurement noise and/or modeling error. So the system equation with noise is as follows,

$$y = X\theta + \epsilon \quad (\text{A.14})$$

ϵ is assumed as a stationary random vector with zero mean value, that is, $E[\epsilon] = 0$. Where $E[.]$ indicates statistical expectation. Furthermore, ϵ is uncorrelated¹ with y and X . Based on these assumptions it can be analyzed how the parameter estimation quality

¹In statistics two real-values random variables are said to be uncorrelated if their covariance is zero

is given by equations A.11 and A.13.

In general, θ and $\hat{\theta}$ are variables whose accuracy can be measured with statistical properties such as bias, error covariance, efficiency and consistency.

To show that $\hat{\theta}$ is unbiased, it has to be shown that $E[\hat{\theta}] = \theta$. Substituting equation A.14 into equation A.11, results in,

$$\hat{\theta} = \theta + (X^T X)^{-1} X^T \epsilon \quad (\text{A.15})$$

Multiplying the expectation term on both sides of equation A.15 and taking $E[\epsilon] = 0$., the result is,

$$E[\hat{\theta}] = E[\theta] + E[(X^T X)^{-1} X^T] E[\epsilon] = \theta \quad (\text{A.16})$$

Similarly it can be shown that $E[\hat{\theta}_w] = 0$.

For the estimate error $\hat{\theta} - \theta$ covariance matrix is,

$$\begin{aligned} \psi &\triangleq E(\hat{\theta} - \theta)(\hat{\theta} - \theta)^T \\ \psi &= E[(X^T X)^{-1} X^T \epsilon][(X^T X)^{-1} X^T \epsilon]^T \\ \psi &= (X^T X)^{-1} X^T E \epsilon \epsilon^T X (X^T X)^{-1} \end{aligned} \quad (\text{A.17})$$

The covariance matrix of the error vector can be defined as R as follows,

$$R = E[\epsilon \epsilon^T], \quad (\text{A.18})$$

Using this the equation for ψ can be reduced to,

$$\psi = (X^T X)^{-1} X^T R X (X^T X)^{-1} \quad (\text{A.19})$$

Following the same procedure, it can be shown that the error covariance of $\hat{\theta}_w$ is,

$$\psi_W = (X^T W X)^{-1} X^T W R W^T X (X^T W X)^{-1} \quad (\text{A.20})$$

If the weighting matrix W is taken as $W = R^{-1}$, then ψ_w can be simplified as,

$$\psi_W = (X^T R^{-1} X)^{-1} = \psi_{MV} \quad (\text{A.21})$$

Then the corresponding estimator $\hat{\theta}_W$ is

$$\hat{\theta}_W = (X^T R^{-1} X)^{-1} X^T R^{-1} y = \hat{\theta}_{MV} \quad (\text{A.22})$$

The Error covariance ψ_{MV} has a very important property. ψ_{MV} is a minimum error covariance matrix, because for any other choice of weighting matrices W ,

$$\psi_{MV} \leq \psi_W \quad (\text{A.23})$$

If the difference $\psi_{MV} - \psi_W$ is a non negative definite value then a positive definite matrix ψ_{MV} is less than or equal to ψ_W . Here MV denotes "Minimum Variance" property.

The estimator $\hat{\theta}_{MV}$ in equation A.22 is known as *minimum variance estimator*, or *Markov estimator*. Thus $\hat{\theta}_{MV}$ is a good linear unbiased estimator.

If the noise $\epsilon(i)$, where $i = 1, 2, \dots$ are ideally distributed and independent with zero mean and variance σ^2 , the covariance R becomes,

$$R = E[\epsilon \epsilon^T] = \sigma^2 I \quad (\text{A.24})$$

In this case, both ψ and ψ_{MV} are identical:

$$\psi = \psi_{MV} = \sigma^2(X^T X)^{-1} \quad (\text{A.25})$$

This implies that the corresponding $LSE\hat{\theta}$ is a minimum variance estimator. $\hat{\theta}$ is called an *efficient estimator*.

It can be shown that the LSE $\hat{\theta}$ is a consistent estimator. Assuming $R = \sigma^2 I$ and rewriting the error covariance matrix ψ as,

$$\psi = \sigma^2(X^T X)^{-1} = \frac{\sigma^2}{m} \left(\frac{1}{m} X^T X \right)^{-1} \quad (\text{A.26})$$

Where m is the number of equations in the vector equation A.14. Assuming that $\lim_{m \rightarrow \infty} [(1/m)X^T X]^{-1} = \Gamma$, where, Γ is a non singular constant matrix. Therefore,

$$\lim_{m \rightarrow +\infty} \psi = \lim_{m \rightarrow +\infty} \frac{\sigma^2}{m} \left(\frac{1}{m} X^T X \right)^{-1} = 0 \quad (\text{A.27})$$

A covariance with zero error means that $\hat{\theta} = \theta$ as $m \rightarrow \infty$. This property of convergence points that $\hat{\theta}$ is a consistent estimator.

It has been shown that the least squares estimator in the presence of white noise is unbiased, efficient, and consistent. Further to be noted that the LSE $\hat{\theta}$ is also identical to the maximum likelihood (MLE) ² when the noise ϵ is Gaussian-distributed.

²This is not going to be discussed in this thesis

A.4 Transfer Function Identification

A.4.1 General Concepts

It is assumed that x_t and y_t represent the input and output signals of a linear system.

x_t and y_t . In a single input, single output (SISO) linear system, a linear filter equation can relate the output series y_t and the input series x_t ,

$$y_t = v(B)x_t + n_t \quad (\text{A.28})$$

Where n_t is the noise series of the system. It is independent of the system input. $v(B) = \sum_{j=-\infty}^{\infty} v_j B^j$ is referred to as the transfer function of filter by Box, Jenkins, and Reinsel [40].

The coefficients v_j in the transfer function model A.28 are often called the impulse response weights. This is also called the impulse response function as a function of j . The transfer function model is said to be stable if the absolute value sum of all the sequence impulse response weights is summable, that is if $\sum |v_j| < \infty$. Thus for a stable system a bounded input will always produce bounded output. The transfer function model is a causal model if $v_j = 0$ for $j < 0$. Thus, in a causal model, the system does not respond to input series until they have been actually applied to the system. So the system's present and past input values are the only ones that affect the present output values. All physical systems are mostly causal and that is why they are also called realizable model. In practice usually the stable and causal models are considered.

$$y_t = v_0 x_t + v_1 x_{t-1} + v_2 x_{t-2} + \dots + n_t$$

$$y_t = v(B)x_t + n_t \quad (\text{A.29})$$

where $v(B) = \sum_{j=0}^{\infty} v_j B^j$, $\sum_{j=0}^{\infty} |v_j| < \infty$ and x_t and n_t are independent. The system is presented in Figure A.2.

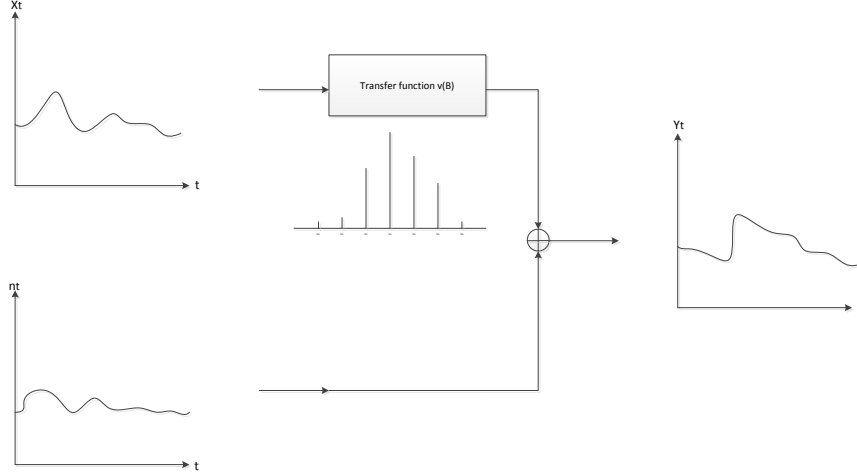


Figure A.2: A Dynamic Transfer Function System.

The purposes of transfer function modeling are to identify and estimate the transfer function $v(B)$ and the noise model for n_t with the available input-output information of x_t and y_t . A complication in this process could be that the information on the x_t and y_t are usually finite and the transfer function $v(B)$ in Equation A.29 can contain infinite number of coefficients. To avoid these difficulties, the transfer function $v(B)$ can be represented in a rational form as Equation A.30,

$$v(b) = \frac{\omega(B)B^b}{\delta(B)} \quad (\text{A.30})$$

Where, $\omega(B) = \omega_0 - \omega_1 B - \dots - \omega_s B^s$, $\delta(B) = 1 - \delta_1 B - \dots - \delta_r B^r$. The b is a parameter that represents delay, defines the actual time lag that elapses before the impulse of the input variable shows an effect to the output variable. For a stable system it is assumed that the roots of $\delta(B) = 0$ are outside the unit circle.

The orders of s, r , and b along with their relationships to the impulse response weights

Table A.1: Impluse reponse weights

Impluse reponse weights	
$v_j = 0$	$j \leq b,$
$v_j = \delta_1 v_{j-1} + \delta_2 v_{j-2} + \dots + \delta_r v_{j-r} + \omega_0$	$j = b,$
$v_j = \delta_1 v_{j-1} + \delta_2 v_{j-2} + \dots + \delta_r v_{j-r} - \omega_{j-b}$	$j = b + 1, b + 2, \dots, b + s,$
$v_j = \delta_1 v_{j-1} + \delta_2 v_{j-2} + \dots + \delta_r v_{j-r},$	$j > b + s$

v_j can be obtained by equating the coefficients of B^j in both sides of the equation,

$$\delta(B)v(B) = \omega(B)B^b$$

or

$$[1 - \delta_1 B - \dots - \delta_r B^r][v_0 + v_1 B + v_2 B^2 + \dots] = [\omega_0 - \omega_1 B - \dots - \omega_s B^s]B^b \quad (\text{A.31})$$

The r impulse response weights $v_{b+s}v_{b+s-1}, \dots, v_{b+s-r+1}$ can be used as starting values for the difference equation,

$$\delta(B)v_j = 0, \quad j > b + s. \quad (\text{A.32})$$

Therefore, the impulse response weights for the system in Equation A.30 consists of the following,

1. b zero weights v_0, v_1, \dots, v_{b-1}
2. $s - r + 1$ weights $v_b, v_{b+1}, \dots, v_{b+s-r}$ that do not follow a fixed pattern.
3. r starting impulse response weights $v_{b+s-r+1}, v_{b+s-r+2}, \dots$, and v_{b+s} .
4. v_j , for $j > b + s$, that follows the pattern give in A.32.

So it is evident that b is determined by $v_j = 0$ for $j < b$ and $v_b \neq 0$. The value r is determined by the pattern of the weights of the impulse response. For any given value

of b , if $r = 0$, then the value s can easily be found using $v_j = 0$ for $j > b + s$; if $r \neq 0$, value of s can be found by finding out where the pattern of decay for impulse response weight begins.

A.4.2 Some Typical Impulse Response Functions

In general, r and s has values which is not more than 2 in most cases. Some typical transfer functions are tabulated as follows,

1. When $r = 0$, the transfer function contains finite number of impulse response weights starting with $v_b = \omega_0$ and ending at $v_{b+s} = -\omega_s$ as shown in table A.2.
2. When $r = 1$, impulse response weights follows an exponential decay starting from v_b if $s = 0$, from v_{b+1} if $s = 1$, and from v_{b+1} if $s = 2$ as shown in Table A.3.

Table A.2: Transfer function for $r=0$

(b,r,s)	Transfer function
(2, 0, 0)	$v(B)x_t = \omega_0 x_{t-2}$
(2, 0, 1)	$v(B)x_t = (\omega_0 - \omega_1 B) x_{t-2}$
(2, 0, 2)	$v(B)x_t = (\omega_0 - \omega_1 B - \omega_2 B^2) x_{t-2}$

Table A.3: Transfer function for r=1

(b,r,s)	Transfer function
(2, 0, 0)	$v(B)x_t = \frac{\omega_0}{1-\delta_1 B}x_{t-2}$
(2, 0, 1)	$v(B)x_t = \left(\frac{\omega_0-\omega_1 B}{1-\delta_1 B}\right)x_{t-2}$
(2, 0, 2)	$v(B)x_t = \frac{\omega_0 - \omega_1 B - \omega_2 B^2}{1 - \delta_1 B}x_{t-2}$

A.4.3 The Cross Correlation Function and Transfer Function

To measure the strength and direction of correlation between two random variables, the cross-correlation function is very useful. If two stochastic process is given as x_t and y_t for $t = 0, \pm 1, \pm 2, \dots$, we can be said that x_t and y_t are jointly stationary if x_t and y_t are both uni-variate stationary processes. The cross covariance function between x_t and y_s , $\text{Cov}(x_t, y_s)$ is a function of time difference ($s - t$) only. In such cases the cross covariance functions can be represented as following,

$$\gamma_{xy}(k) = E[(x_t - \mu_x)][(y_{t+k} - \mu_y)] \quad (\text{A.33})$$

for $k = 0, \pm 1, \pm 2, \dots$, where $\mu_x = E(x_t)$ and $\mu_y = E(y_t)$. the following cross-correlation (CCF) can be obtained,

$$\rho_{xy}(k) = \frac{\gamma_{xy}(k)}{\sigma_x \sigma_y} \quad (\text{A.34})$$

for $k = 0, \pm 1, \pm 2, \dots$, where δ_x and δ_y are standard deviation of x_t and y_t . It is noteworthy that the cross-covariance function $\delta_{xy}(k)$ and cross-correlation functions $\rho_{xy}(k)$ are generalizations of autocovariances and autocorrelation functions. This is because

$\delta_{xx}(k) = \delta_x(k)$ and $\rho_{xx} = \rho_x(k)$. The cross-correlation function is not symmetric, i.e., $\rho_{xy}(k) \neq \rho_{xy}(-k)$. But in the other side as, $\gamma_{xy}(k) = E(x_t - \mu_x)(y_{t+k} - \mu_y) = E(y_{t+k} - \mu_y)(x_t - \mu_x) = \gamma_{xy}(-k)$, it is true that $\rho_{xy}(k) = \rho_{xy}(-k)$. So it can be said that the CCF not only measures the strength of an association but also its direction.

A.4.4 The Relationship Between the Cross-Correlation Function and the Transfer Function

At time $t + k$, the transfer function model at A.29 can be represented as following,

$$y_{t+k} = v_0 x_t + k + v_1 x_{t+k-1} + v_2 x_{t+k-2} + \dots + n_{t+k} \quad (\text{A.35})$$

It can be safely assumed that $\mu_x = 0$ and $\mu_y = 0$. If both sides are multiplied with x_t at A.35 and taking expectations,

$$\gamma_{xy}(k) = v_0 \gamma_{xx}(k) + v_1 \gamma_{xx}(k-1) + v_2 \gamma_{xx}(k-2) + \dots, \quad (\text{A.36})$$

for all values of k , $\gamma_{xn}(k) = 0$, Hence,

$$\rho_{xy}(k) = \frac{\sigma_x}{\sigma_y} [v_0 \rho_x(k) + v_1 \rho_x(k-1) + v_2 \rho_x(k-2) + \dots] \quad (\text{A.37})$$

The auto correlation structure of the input series x_t effects the relationship between the CCF, $\rho_{xy}(k)$ and the impulse response function v_j . Even if $r = 0$ in (4.29) and if the transfer function $v(B)$ contains only a finite number of impulse response weights, the use of A.37 to form a system of equations to solve for v_j as a function of $\rho_{xy}(k)$ and $\rho_x(k)$ is difficult. The contamination by the auto correlation structure of the input series x_t to variance and covariance of the sample estimate of $\rho_{xy}(k)$ is clear from A.37, which makes

the identification of both $\rho_{xy}(k)$ and v_k difficult.

If a white noise is provided as the input series which implies $\rho_x(k) = 0$ for $k \neq 0$, then A.37 can be reduced to,

$$v_k = \frac{\sigma_y}{\sigma_x} \rho_{xy}(k) \quad (\text{A.38})$$

Therefore, the impulse response function v_k is directly proportional to the cross-correlation function $\rho_{xy}(k)$. Some observations can be made as following,

1. When both x_t and y_t are bivariate stationary process at the same instant then only the CCF, $\rho_{xy}(k)$ is defined.
2. In the general form of transfer function model,

$$y_t = v(B)x_t + n_t \quad (\text{A.39})$$

it can be assumed that the input series x_t follows an Auto Regressive Moving Average process, thus,

$$\phi_x(B)x_t = \theta_x(B)\alpha_t$$

Here α_t is considered as white noise. The series α_t ,

$$\frac{\phi_x(B)}{\theta_x(B)}x_t \quad (\text{A.40})$$

Equation (4.40) is often called the prewhitened input series. Same prewhitening transformation can be applied to the output series y_t , and a filtered output series is obtained from there,

$$\beta_t = \frac{\phi_x(B)}{\theta_x(B)}y_t \quad (\text{A.41})$$

If the right hand side of (4.41) is assumed as $\varepsilon_t = \theta_x^{-1}(B)n_t$, the transfer function model in A.39 becomes,

$$\beta_t = v(B)\alpha_t + \varepsilon_t \quad (\text{A.42})$$

For this transfer function the impulse response weights v_j can be found as,

$$v_k = \frac{\sigma_\beta}{\sigma_\alpha} \rho_{\alpha\beta}(k) \quad (\text{A.43})$$

This is helpful for the fundamental steps of the identification of transfer function models to be discussed in the later section.

A.4.5 Construction of Transfer Function Models.

A.4.5.1 Sample Cross-Correlation Function

For a known set of time series data x_t and y_t , $1 \leq t \leq n$, the cross correlation function becomes,

$$\rho_{xy}(k) = \frac{\gamma_{xy}(k)}{\sigma_x \sigma_y}, k = 0, \pm 1, \pm 2, \dots, \quad (\text{A.44})$$

can be estimated by the sample cross-correlation function,

$$\hat{\rho}_{xy}(k) = \frac{\hat{\gamma}_{xy}(k)}{S_x S_y}, k = 0, \pm 1, \pm 2, \dots, \quad (\text{A.45})$$

where,

$$\hat{\gamma}_{xy}(k) = \begin{cases} \frac{1}{n} \sum_{t=1}^{n-k} (x_t - \bar{x})(y_{t+k} - \bar{y}), & k \geq 0, \\ \frac{1}{n} \sum_{t=1-k}^n (x_t - \bar{x})(y_{t+k} - \bar{y}), & k < 0, \end{cases} \quad (\text{A.46})$$

$$S_x = \sqrt{\hat{\gamma}_{xx}(0)}, S_y = \sqrt{\hat{\gamma}_{yy}(0)}, \quad (\text{A.47})$$

Here \bar{x} and \bar{y} are the sample means of the input-output series x_t and y_t .

In order to test if some values of the $\rho_{xy}(k)$ are zero, The sample CCF $\rho_{xy}(k)$ is compared with their standard errors. Between two sample cross-correlation $\rho_{xy}(k)$ and $\rho_{xy}(k+j)$ under normal assumptions Bartlett [41] derived the approximate variance and covariance. The covariance is given by,

$$\begin{aligned} Cov[\hat{\rho}_{xy}(k), \hat{\rho}_{xy}(k+j)] &= (n-k)^{-1} \sum_{i=-\infty}^{\infty} \{ \rho_{xx}(i)\rho_{yy}(i+j) + \rho_{xy}(i+k+j)\rho_{xy}(k-i) \\ &+ \rho_{xy}(k)\rho_{xy}(k+j) \left[\rho_{xy}^2(i) + \frac{1}{2}\rho_{xx}^2(i) + \frac{1}{2}\rho_{yy}^2(i) \right] \\ &- \rho_{xy}(k) [\rho_{xx}(i+k+j) + \rho_{xy}(-i)\rho_{yy}(i+k+j)] \\ &- \rho_{xy}(k+j) [\rho_{xx}(i)\rho_{xy}(i+k) + \rho_{xy}(-i)\rho_{yy}(i+k)] \} \end{aligned}$$

Hence,

$$\begin{aligned} Var[\hat{\rho}_{xy}(k)] &= (n-k)^{-1} \sum_{i=-\infty}^{\infty} \{ \rho_{xx}(i)\rho_{yy}(i) + \rho_{xy}(k+i)\rho_{xy}(k-i) \\ &+ \rho_{xy}^2(k) \left[\rho_{xy}^2(i) + \frac{1}{2}\rho_{xx}^2(i) + \frac{1}{2}\rho_{yy}^2(i) \right] \\ &- 2\rho_{xy}(k) [\rho_{xx}(i)\rho_{xy}(i+k) + \rho_{xy}(-i)\rho_{yy}(i+k)] \} \end{aligned}$$

With the hypothesis that the series x_t and y_t are uncorrelated and x_t is white noise series, the covariance equation becomes,

$$Cov[\hat{\rho}_{xy}(k), \hat{\rho}_{xy}(k+j)] = (n-k)^{-1} \rho_{yy}(j) \quad (\text{A.48})$$

It follows that

$$Var[\hat{\rho}_{xy}(k)] = (n-k)^{-1} \quad (\text{A.49})$$

So by comparing the sample CCF $\hat{\rho}_{xy}(k)$ with their approximate standard errors $1/\sqrt{(n-k)}$ it can be tested that the series x_t and y_t are not cross-correlated under the condition that the series x_t is white noise.

In reality the x_t series is not white noise, thus it has to be prewhitened and also filter the output series, as will be shown in the next section.

A.4.5.2 Identification of Transfer Function Models

Refer to the discussions from the previous sections the following steps can be followed to obtain the transfer function $v(B)$,

1. Prewhitening of the input series,

$$\phi_x(B)x_t = \theta_x(B)\alpha_t, \quad (\text{A.50})$$

Thus,

$$\alpha_t = \frac{\phi_x(B)}{\theta_x(B)} y_t \quad (\text{A.51})$$

where, α_t is a white noise series with mean zero and variance σ_α^2

2. Calculation of the filtered output series. That is transformation of the output series

y_t using the above prewhitening model to generate the series,

$$\beta_t = \frac{\phi_x(B)}{\theta_x(B)} y_t \quad (\text{A.52})$$

3. Calculation of the sample CCF, $\hat{\rho}_{\alpha\beta}(k)$ between α_t and β_t to estimate v_k :

$$\hat{v}_k = \frac{\hat{\sigma}_\beta}{\hat{\sigma}_\alpha} \hat{\rho}_{\alpha\beta}(k) \quad (\text{A.53})$$

4. Identification of b , $\delta(B) = (1 - \delta_1 B - \dots - \delta_r B^r)$, and $\omega(B) = (\omega_0 - \omega_1 B - \dots - \omega_s B^s)$ by matching the pattern of \hat{v}_k with the already known theoretical patterns of the v_k as discussed in section A.4.1 and A.4.2. Preliminary estimates of $\hat{\omega}_j$ and $\hat{\delta}_j$ can be found from their relationship with v_k once b, r , and s are chosen as shown in A.31. Thus a preliminary estimate of the transfer function $v(B)$ can be found as,

$$\hat{v}(B) = \frac{\hat{\omega}(B)}{\hat{\delta}(B)} B^b \quad (\text{A.54})$$

Once the preliminary model of the transfer function is identified, the noise series estimation can be done,

$$\begin{aligned} \hat{n}_t &= y_t - \hat{v}(B)x_t \\ \hat{n}_t &= y_t - \frac{\hat{\omega}(B)}{\hat{\delta}(B)} B^b x_t \end{aligned} \quad (\text{A.55})$$

The appropriate model for the noise can be identified by examining its sample ACF and PACF or by other univariate tools for time series identification, thus,

$$\phi(B)n_t = \theta(B)a_t \quad (\text{A.56})$$

Remarks Combining A.54 and A.56 the following transfer function model can be obtained,

$$y_t = \frac{\omega(B)}{\delta(B)}x_{t-b} + \frac{\theta(B)}{\phi(B)}a_t \quad (\text{A.57})$$

Some important points are as below,

1. In the construction of the model, it is assumed that the variables y_t , x_t , and n_t are all stationary, therefore for non-stationary variables some process has to be followed to achieve stationarity.
2. In the identification process of the transfer function $v(B)$ the input series is prewhitened. That prewhitened model is applied to filter the output series, but that does not necessarily whiten it. This method of constructing a causal transfer function model is simple and regularly used.

A.4.5.3 Estimation of Transfer Function Models

An initial tentative transfer function model can be identified. Then from that initial identified model,

$$y_t = \frac{\omega(B)}{\delta(B)}x_{t-b} + \frac{\theta(B)}{\phi(B)}a_t \quad (\text{A.58})$$

The parameters $\delta = (\delta_1, \dots, \delta_r)'$, $\omega = (\omega_0, \omega_1, \dots, \omega_s)'$, $\phi = (\phi_1, \dots, \phi_p)'$, $\theta = (\theta_1, \dots, \theta_q)'$, and σ_a^2 are the ones which is estimated. So A.58 can be re-written as,

$$\delta(B)\phi(B)y_t = \phi(B)\omega(B)x_{t-b} + \delta(B)\theta(B)a_t \quad (\text{A.59})$$

To write this in a compact form, it can be assumed that,

$$\begin{aligned}
 c(B) &= \delta(B)\phi(B) \\
 &= (1 - \delta_1(B) - \dots - \delta_r B^r)(1 - \phi_1 B - \dots - \phi_p B^p) \\
 &= (1 - c_1 B - c_2 B^2 - \dots - c_{p+r} B^{p+r}),
 \end{aligned}$$

$$\begin{aligned}
 d(B) &= \phi(B)\omega(B) \\
 &= (1 - \phi_1(B) - \dots - \phi_p B^p)(\omega_0 - \omega_1 B - \dots - \omega_s B^s) \\
 &= (d_0 - d_1 B - d_2 B^2 - \dots - d_{p+s} B^{p+s})
 \end{aligned}$$

and,

$$\begin{aligned}
 e(B) &= \delta(B)\theta(B) \\
 &= (1 - \delta_1(B) - \dots - \delta_r B^r)(1 - \theta_1 B - \dots - \theta_q B^q) \\
 &= (1 - e_1 - e_2 B - \dots - e_{r+q} B^{r+q})
 \end{aligned}$$

Thus,

$$\begin{aligned}
 a_t = & y_t - c_1 y_{t-1} - \dots - c_{p+r} y_{t-p-r} - d_0 x_{t-b} + d_1 x_{t-b-1} \\
 & + \dots + d_{p+s} x_{t-b-p-s} + e_1 a_{t-1} + \dots + e_{r+q} a_{t-r-q}
 \end{aligned} \tag{A.60}$$

Where c_i , d_j , and e_k are functions of $\delta_i, \omega_j, \phi_k$, and θ_i . A conditional likelihood

function can be obtained under the assumption that a_t are $N(0, \delta_a^2)$ white noise series, as follows,

$$L(\delta, \omega, \phi, \theta, \sigma_a^2 | b, x, y, x_0, y_0, a_0) = (2\pi\sigma_a^2)^{-n/2} \exp \left[-\frac{1}{2\sigma_a^2 \sum_{t=1}^n a_t^2} \right] \quad (\text{A.61})$$

Here, x_0, y_0, a_0 are initial starting values for computing a_t from A.60.

To estimate the parameters $\delta, \omega, \phi, \theta, \sigma_a^2$ various estimation methods can be used. For example, by setting the unknown a's equal to their conditional expected values or zero, non linear least squares of these parameters can be found by minimizing,

$$S(\delta, \omega, \phi, \theta | b) = \sum_{t=t_0}^n a_t^2 \quad (\text{A.62})$$

where, $t_0 = \max[p + r + 1, b + p + s + 1]$,

It is assumed that b is known. For given values of r,s,p, and q, if it is needed also to estimate b, then A.62 can be optimized for a likely range of values of b. Then the value of b can be selected so that gives the overall minimum of the sum of squares.

A.5 About PSS/E Simulation Program

Power System Simulation for Engineering (PSS/E) is composed of a comprehensive set of programs for studies of power system transmission network and generation performance in both steady-state and dynamic conditions. There are two primary simulations used,

1. For the steady state analysis.
2. For dynamic simulations.

This simulation program can be used for several types of analyses, which includes:

1. Power flow analysis.
2. Balanced and unbalanced faults.
3. Network equivalent construction.
4. Dynamic simulation.

PSS/E is capable of providing the users with a wide range of auxiliary programs for installation in addition with the steady-state and dynamic analyses. This software has a graphical user interface. Which contains various functionality of state analysis; that includes load flow, fault analysis, optimal power flow, equivalency, and switching studies.

In addition, to the steady-state and dynamic analyses, PSS/E also provides the user with a wide range of auxiliary programs for installation, data input, output, manipulations and preparation.

Bibliography

- [1] BJ Kirby, J Dyer, C Martinez, Rahmat A Shoureshi, R Guttromson, and J Dagle. *Frequency control concerns in the North American electric power system*. United States. Department of Energy, 2003.
- [2] HM Dimond and GS Lunge. Continuous load-frequency control for interconnected power systems. *American Institute of Electrical Engineers, Transactions of the*, 67(2):1483–1490, 1948.
- [3] Stan Mark Kaplan. Electric power transmission: background and policy issues. *Congressional Research Service, Washington DC*, 2009.
- [4] NERC Resources Subcommittee. Balancing and frequency control, January 2011.
- [5] Definitions of terminology for automatic generation control on electric power systems. Nov 1965.
- [6] North American Electric Reliability Corporation, corporate website (www.nerc.com).
- [7] Nasser Jaleeli and Louis S VanSlyck. NERC’s new control performance standards. *Power Systems, IEEE Transactions on*, 14(3):1092–1099, 1999.

- [8] Maojun Yao, Raymond R Shoults, and Randy Kelm. AGC logic based on NERC's new control performance standard and disturbance control standard. *Power Systems, IEEE Transactions on*, 15(2):852–857, 2000.
- [9] N.Jaleeli and L.S. VanSlyck. Control performance standards and procedures. *Power Delivery and Utilization, Technical Report EPRI*, June 1997.
- [10] Thusitha Wickramasinghe. Estimation of frequency control performance using probability distribution of load change. Master's thesis, University of Manitoba, 2010.
- [11] T Jayasekara, UD Annakkage, R Karki, and B Jayasekara. Estimation of frequency control performance using probability distribution of load change. In *Electrical and Computer Engineering (CCECE), 2013 26th Annual IEEE Canadian Conference on*, pages 1–6. IEEE, 2013.
- [12] Nicolas Maruejols, Thibault Margotin, Marc Trotignon, Pierre L Dupuis, and J-M Tesson. Measurement of the load frequency control system service: comparison between american and european indicators. *Power Systems, IEEE Transactions on*, 15(4):1382–1387, 2000.
- [13] Ch Roethlisberger, A.M. Gole, U.D. Annakkage, and G. Andersson. Model identification for spinning reserve management. In *Electrical and Computer Engineering, 2006. CCECE '06. Canadian Conference on*, pages 2294–2298, May 2006.
- [14] Prabha Kundur, Neal J Balu, and Mark G Lauby. *Power system stability and control*, volume 7. McGraw-hill New York, 1994.
- [15] Olle Ingemar Elgerd. *Electric energy systems theory: an introduction*. Tata McGraw-Hill Education, 1983.

- [16] Leon K Kirchmayer and NL MEYRICK. *Economic control of interconnected systems*. Wiley New York, NY, 1959.
- [17] Charles Edward Fosha and Olle I Elgerd. The megawatt-frequency control problem: a new approach via optimal control theory. *Power Apparatus and Systems, IEEE Transactions on*, (4):563–577, 1970.
- [18] Olle I. Elgerd and C.E. Fosha. Optimum megawatt-frequency control of multiarea electric energy systems. *Power Apparatus and Systems, IEEE Transactions on*, PAS-89(4), April 1970.
- [19] C. Concordia, L. K. Kirchmayer, and E. A. Szymanski. Effect of speed-governor dead band on tie-line power and frequency control performance. *Power Apparatus and Systems, Part III. Transactions of the American Institute of Electrical Engineers*, 76(3):429–434, April 1957.
- [20] Nasser Jaleeli, Louis S VanSlyck, Donald N Ewart, Lester H Fink, and Arthur G Hoffmann. Understanding automatic generation control. *Power Systems, IEEE Transactions on*, 7(3):1106–1122, 1992.
- [21] Crary Concordia, SB Crary, and EE Parker. Effect of prime-mover speed governor characteristics on power-system frequency variations and tie-line power swings. *Electrical Engineering*, 60(6):559–567, 1941.
- [22] C Concordia and LK Kirchmayer. Tie-line power and frequency control of electric power systems [includes discussion]. *Power apparatus and systems, part iii. transactions of the american institute of electrical engineers*, 72(2), 1953.
- [23] Allen J Wood and Bruce F Wollenberg. *Power generation, operation, and control*. John Wiley & Sons, 2012.

- [24] Yann G Rebours, Daniel S Kirschen, Marc Trotignon, and Sébastien Rossignol. A survey of frequency and voltage control ancillary servicespart i: Technical features. *Power Systems, IEEE Transactions on*, 22(1):350–357, 2007.
- [25] Roger L King, Minh-Luan Ngo, and Rogelio Luck. Interconnected system frequency response. In *System Theory, 1996., Proceedings of the Twenty-Eighth Southeastern Symposium on*, pages 306–310. IEEE, 1996.
- [26] Nathan Cohn. Some aspects of tie-line bias control on interconnected power systems. *AIEE Trans*, 75(2):1415–1428, 1957.
- [27] Nasser Jaleeli and Louis S VanSlyck. Tie-line bias prioritized energy control. *Power Systems, IEEE Transactions on*, 10(1):51–59, 1995.
- [28] Nathan Cohn. *Control of generation and power flow on interconnected power systems*. J. Wiley, 1971.
- [29] Nathan Cohn. Considerations in the regulation of interconnected areas. *Power Apparatus and Systems, IEEE Transactions on*, (12):1527–1538, 1967.
- [30] M-LD Ngo, Roger L King, and Rogelio Luck. Implications of frequency bias settings on agc. In *System Theory, 1995., Proceedings of the Twenty-Seventh Southeastern Symposium on*, pages 83–86. IEEE, 1995.
- [31] NERC committee. Bal-001-1 real power balancing control performance, 2014.
- [32] F. Ding. System identification, part a: Introduction to the identification,. *Journal of Nanjing University of Information Science and Technology: Natural Science edition*, 3:1–22, 2011.

- [33] H. Cui Z. Pang. MATLAB simulation of system identification and adaptive control,. *Beijing National Defense Industry Press*, 1:2–4, 2009.
- [34] D. Liu. System identification methods and applications,. *Beijing National Defense Industry Press*, 1:2–4, 2010.
- [35] Tien C Hsia. System identification. 1977.
- [36] MATLAB Users Guide. The Wikipedia website, 1998.
- [37] MATLAB Users Guide. The Mathworks website, 1998.
- [38] UD Annakkage, DA Jacobson, and D Muthumuni. Method for studying and mitigating the effects of wind variability on frequency regulation. In *Integration of Wide-Scale Renewable Resources Into the Power Delivery System, 2009 CIGRE/IEEE PES Joint Symposium*, pages 1–1. IEEE, 2009.
- [39] Li Fu and Pengfei Li. The research survey of system identification method. In *Intelligent Human-Machine Systems and Cybernetics (IHMSC), 2013 5th International Conference on*, volume 2, pages 397–401. IEEE, Aug 2013.
- [40] George EP Box, Gwilym M Jenkins, and Gregory C Reinsel. *Time series analysis: forecasting and control*. John Wiley & Sons, 2013.
- [41] Maurice S Bartlett. Stochastic processes. *Cambridge University Press*. and Kendall, DG (1951). *On the use of the characteristic functional in the analysis of some stochastic processes occurring in physics and biology*. *Proc. Camb. Phil. Soc*, 47:65–76, 1955.